Electronic Supplementary Material (ESI) for Organic Chemistry Frontiers.

Supporting Information

Fluorescent visualization of cucurbit[8]uril-triggered dynamic host-guest assemblies

Xiaodong Zhang, Tao Sun and Xin-Long Ni*

Key Laboratory of Macrocyclic and Supramolecular Chemistry of Guizhou Province, Guizhou University, Guiyang, 550025, China
E-mail: longni333@163.com

Materials and methods

The solvents and the reagents were purified and dried by usual methods prior to use. Reagents purchased from commercial suppliers were used as received. ^{1}H NMR spectra were measured on a Bruker Avance NEO 600 MHz NMR Spectrometer or JNM-ECZ400 MHz nuclear magnetic resonance (NMR) spectrometer. UV-vis spectra were recorded on an Agilent-8453 spectrophotometer. Fluorescence spectra measurements were performed on a Varian Cary Eclipse fluorescence spectrophotometer equipped with a xenon discharge lamp. Fluorescence lifetime and quantum yield were obtained with an Edinburgh Instrument FLS 980 fluorospectrometer. Isothermal titration calorimetry (ITC) was carried out using a Nano ITC (TA, USA), isothermal titration calorimeter at 25 ℃, computer simulations were performed using the Nano ITC analyze software.

Synthesis of guests

Q[8] and guests were synthesized according to the reported literatures.[1,2] For example, as a typically experiment, a mixture containing 4-vinylpyridine (2.5 mmol), 1,4-Dibromobenzene, 2,5-Dibromotoluene or 1,4-Dibromo-2,5-dimethylbenzene (1 mmol), $(PPh_3)_2PdCl_2$ (0.02 mmol), K_2CO_3 (2 mmol), and DMF (3 mL) was added into a 38 mL Schlenk tube. The tube was evacuated and flushed with nitrogen three times. The mixture was then heated at 120 ℃ for 18 h and then cooled to ambient temperature. The residue formed was dissolved in H_2O and extracted with CH_2Cl_2 (3 × 15 mL). The combined organic layers were washed with brine, dried over Na_2SO_4, and concentrated in vacuo. The resulting solid was purified by flash chromatography on silica gel to give **OPV-H, OPV-Me** or **OPV-2Me**. ^{1}H NMR spectrum of those compounds are shown in Fig. S15.

A mixture containing of **OPV-H**, **OPV-Me** or **OPV-2Me** (1.0 mmol) and haloalkane (4.0 mmol) in DMF (6.0 mL) and was heated to 100 ^{o}C for 24 hours. Then the reaction mixture was cooled and an excess amount of acetone (100 mL) was added the solution. The precipitate was filtered and washed with petroleum ether and acetone to give rise to solid. ^{1}H NMR spectrum of those compounds are shown in Figs. S16-S22.

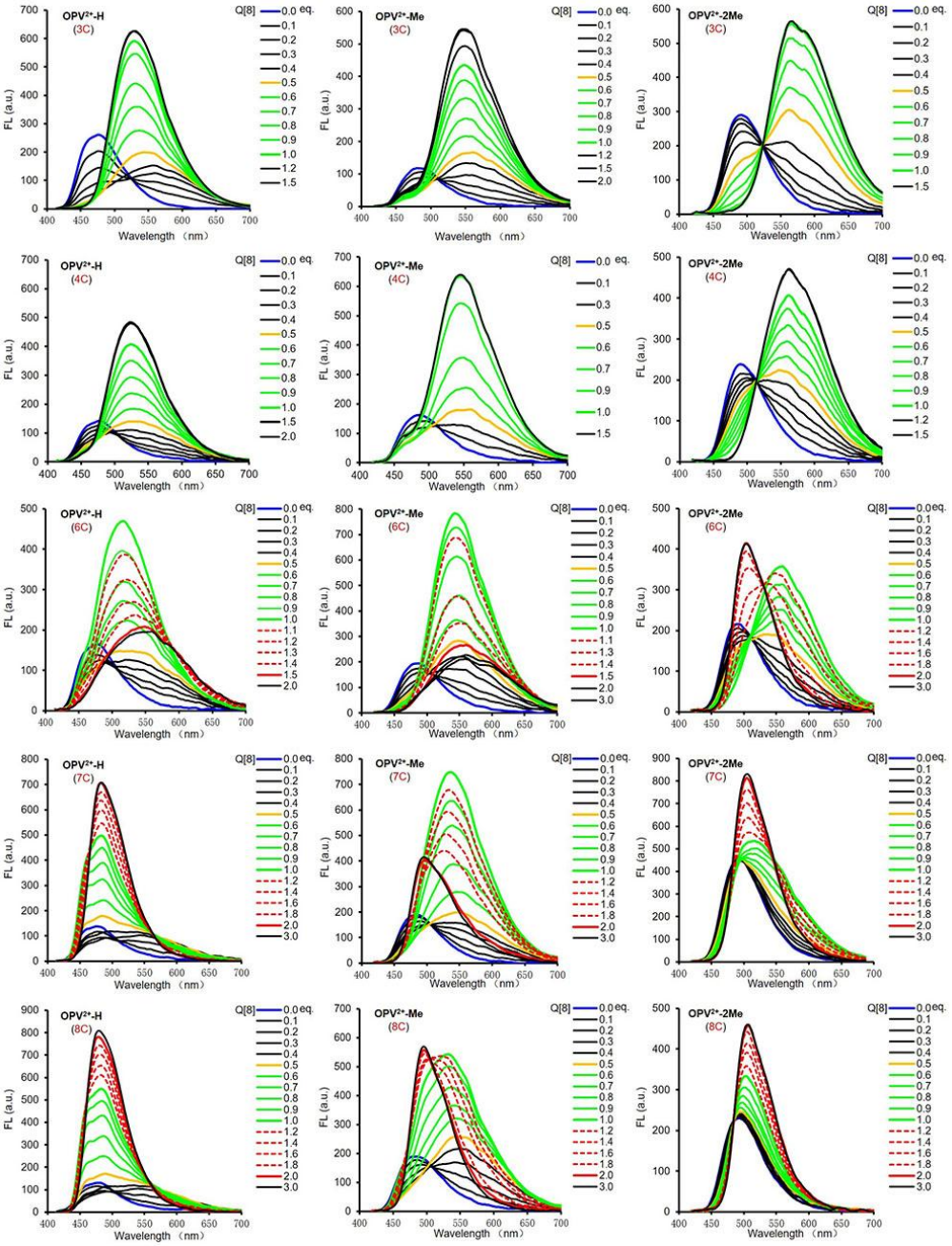
OPV²⁺-H (3C)
OPV²⁺-Me (3C)
OPV²⁺-2Me (3C)
OPV²⁺-H (4C)
OPV²⁺-Me (4C)
OPV²⁺-2Me (4C)
OPV²⁺-H (6C)
OPV²⁺-Me (6C)
OPV²⁺-2Me (6C)
OPV²⁺-H (7C)
OPV²⁺-Me (7C)
OPV²⁺-2Me (7C)
OPV²⁺-H (8C)
OPV²⁺-Me (8C)
OPV²⁺-2Me (8C)
FL (a.u.)
Wavelength (nm)
Q[8] 0.0 eq.

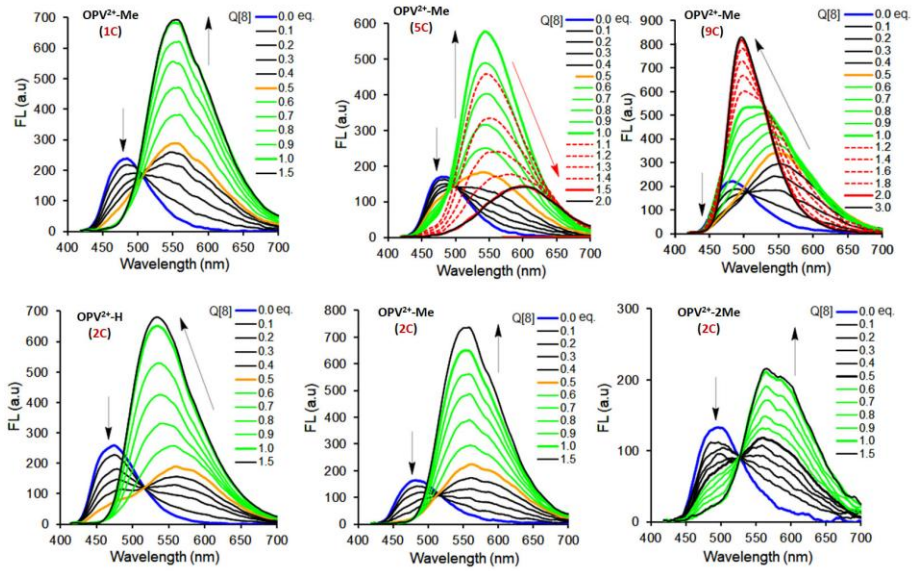

Fig. S1 Fluorescence spectra changes of **OPV^{2+}** core based guests (each of 10.0 μM in aqueous solution, pH 7.2) in the presence of increasing concentrations of Q[8] host. (λ_{ex} = 400 nm)

Table S1 Summarized maximum emission wavelength (nm) of Fig. S1 and Fig.1.

Sample	Free	0.5 eq.	1.0 eq.	1.5 eq.	2.0 eq.
OPV^{2+}-H（1C）	474	565	565		
OPV^{2+}-Me（1C）	485	555	555		
OPV^{2+}-2Me（1C）	482	560	560		
OPV^{2+}-H（2C）	475	560	535		
OPV^{2+}-Me（2C）	483	561	552		
OPV^{2+}-2Me（2C）	483	560	565		
OPV^{2+}-H（3C）	477	550	530		
OPV^{2+}-Me（3C）	482	561	545		
OPV^{2+}-2Me（3C）	482	562	568		
OPV^{2+}-H（4C）	475	542	524		
OPV^{2+}-Me（4C）	485	559	546		
OPV^{2+}-2Me（4C）	482	546	561		
OPV^{2+}-H（5C）	475	547	522	550	
OPV^{2+}-Me（5C）	484	542	543	604	
OPV^{2+}-2Me（5C）	486	549	559		504
OPV^{2+}-H（6C）	478	548	516	548	
OPV^{2+}-Me（6C）	483	547	543	559	
OPV^{2+}-2Me（6C）	485	557	559		504
OPV^{2+}-H（7C）	474	550	494		485
OPV^{2+}-Me（7C）	485	549	536		496
OPV^{2+}-2Me（7C）	483	497	510		510
OPV^{2+}-H（8C）	476	550	498		483
OPV^{2+}-Me（8C）	485	549	533		496
OPV^{2+}-2Me（8C）	483	493	508		508
OPV^{2+}-H（9C）	477	550	489		479
OPV^{2+}-Me（9C）	483	549	515		496
OPV^{2+}-2Me（9C）	483	492	510		510

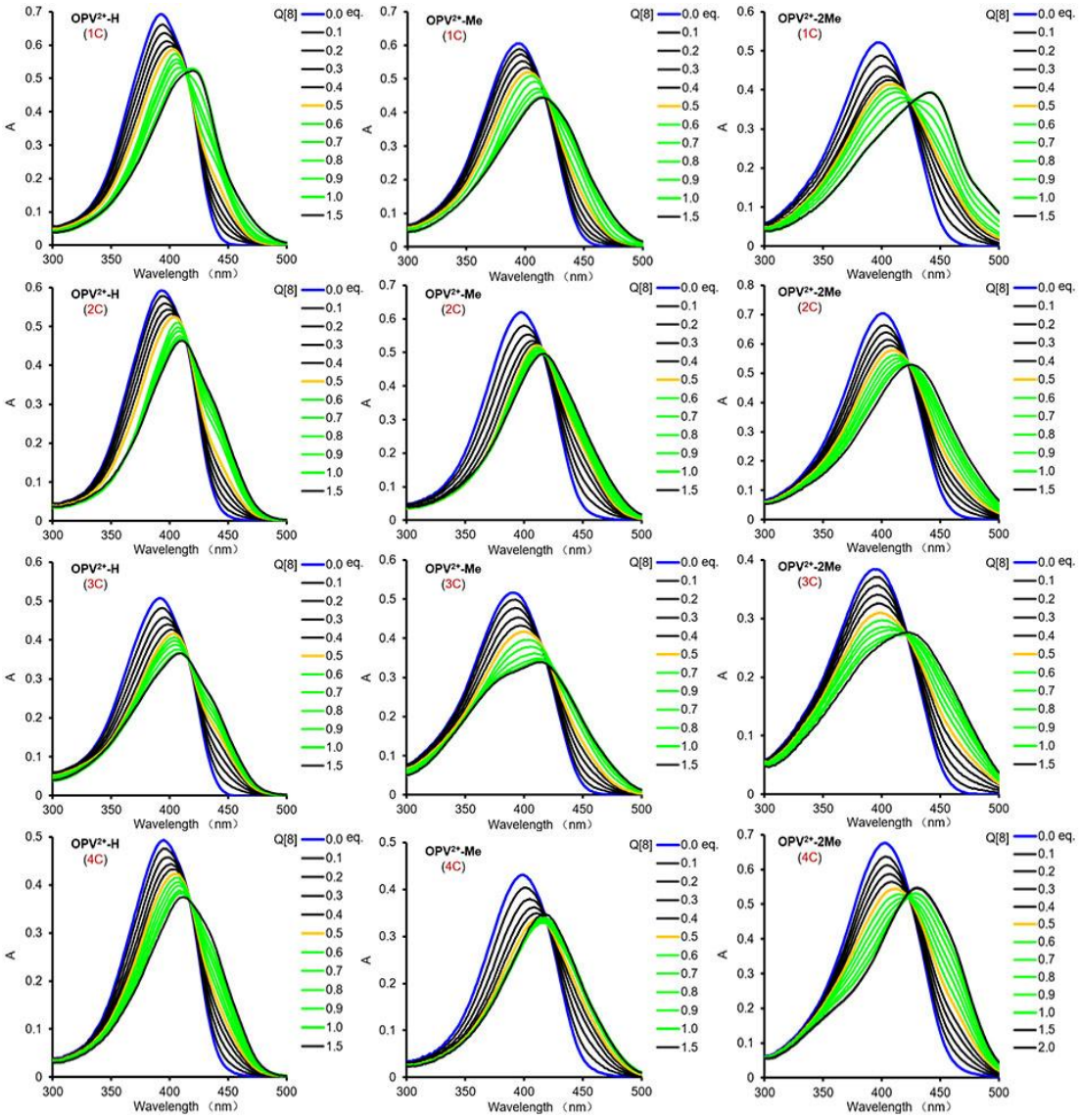

Fig. S2 UV-vis spectra changes of **OPV**$^{2+}$ core based guests (1C-4C, each of 10.0 μM in aqueous solution, pH 7.2) in the presence of increasing concentrations of Q[8] host.

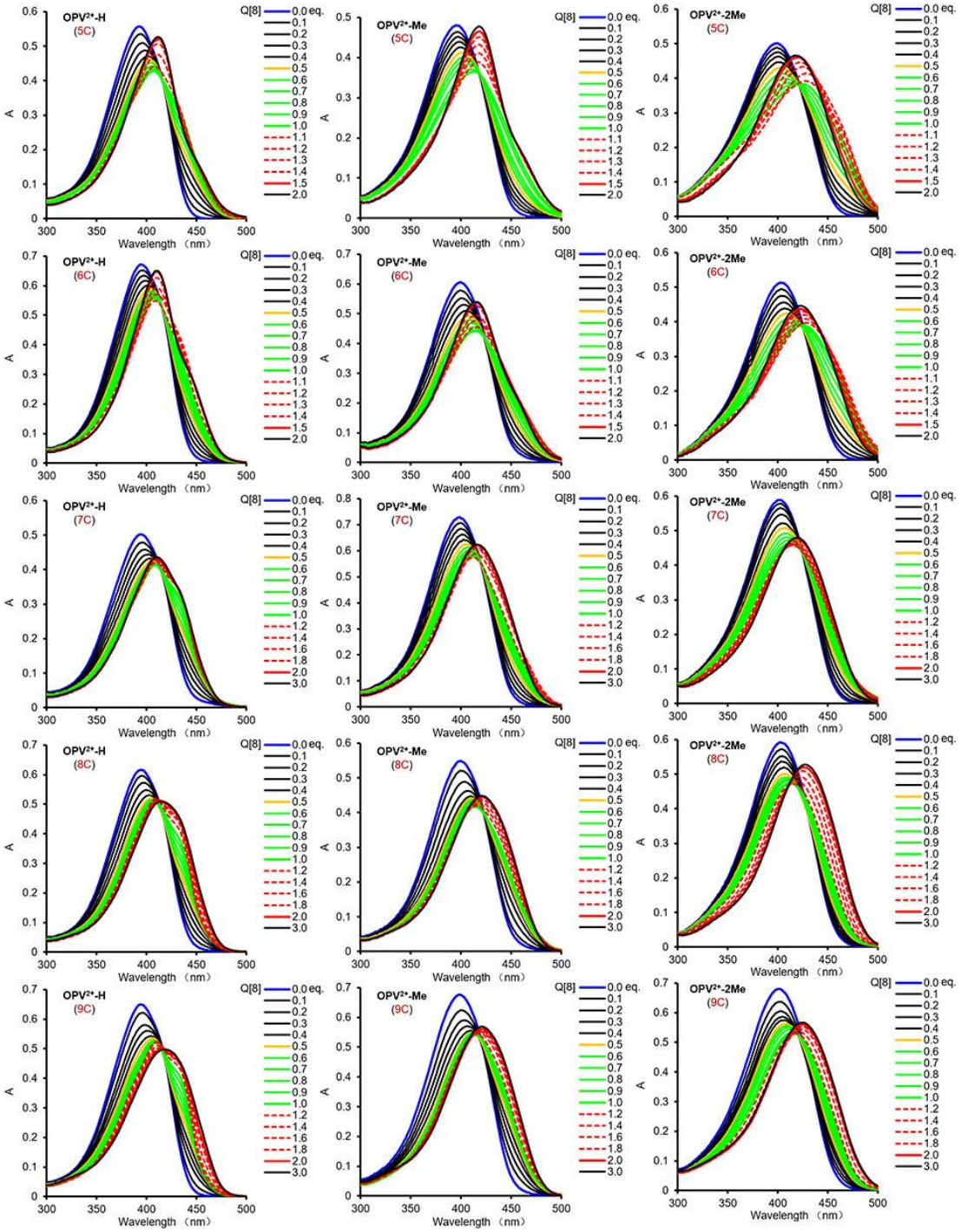

Fig. S3 UV-vis spectra changes of **OPV**$^{2+}$ core based guests (5C-9C, each of 10.0 μM in aqueous solution, pH 7.2) in the presence of increasing concentrations of Q[8] host.

Fig. S4 ^{1}H NMR spectrum of **OPV^{2+}-H** (1C-9C) with different concentration of Q[8].

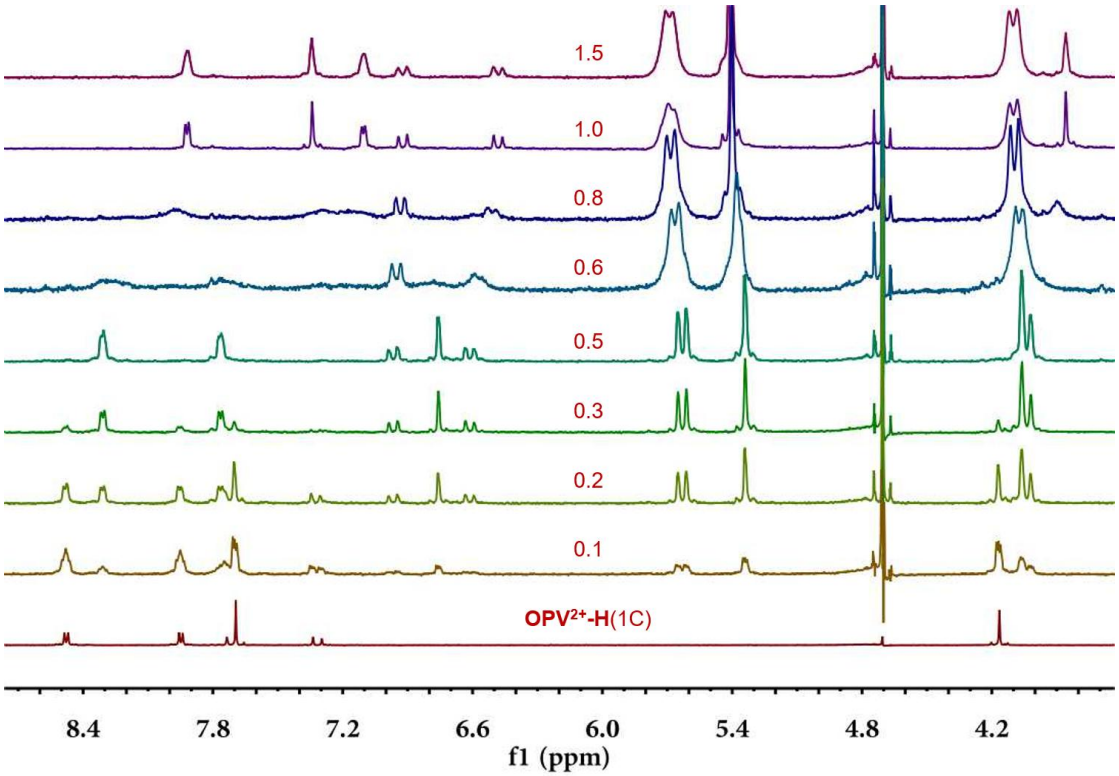

Fig. S4-1 ^{1}H NMR spectrum of **OPV^{2+}-H** (1C) (1.0 mM in D_2O) with different concentration of Q[8] (0.1-1.5 eq.).

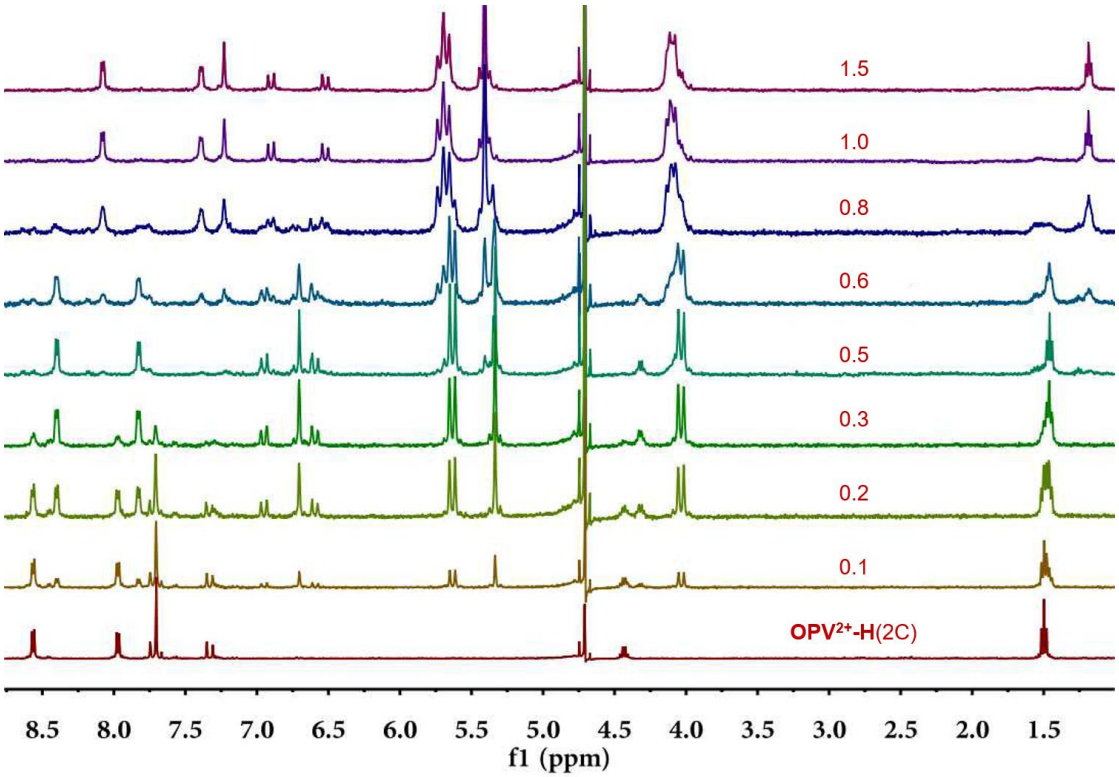

Fig. S4-2 ^{1}H NMR spectrum of **OPV^{2+}-H** (2C) (1.0 mM in D_2O) with different concentration of Q[8] (0.1-1.5 eq.).

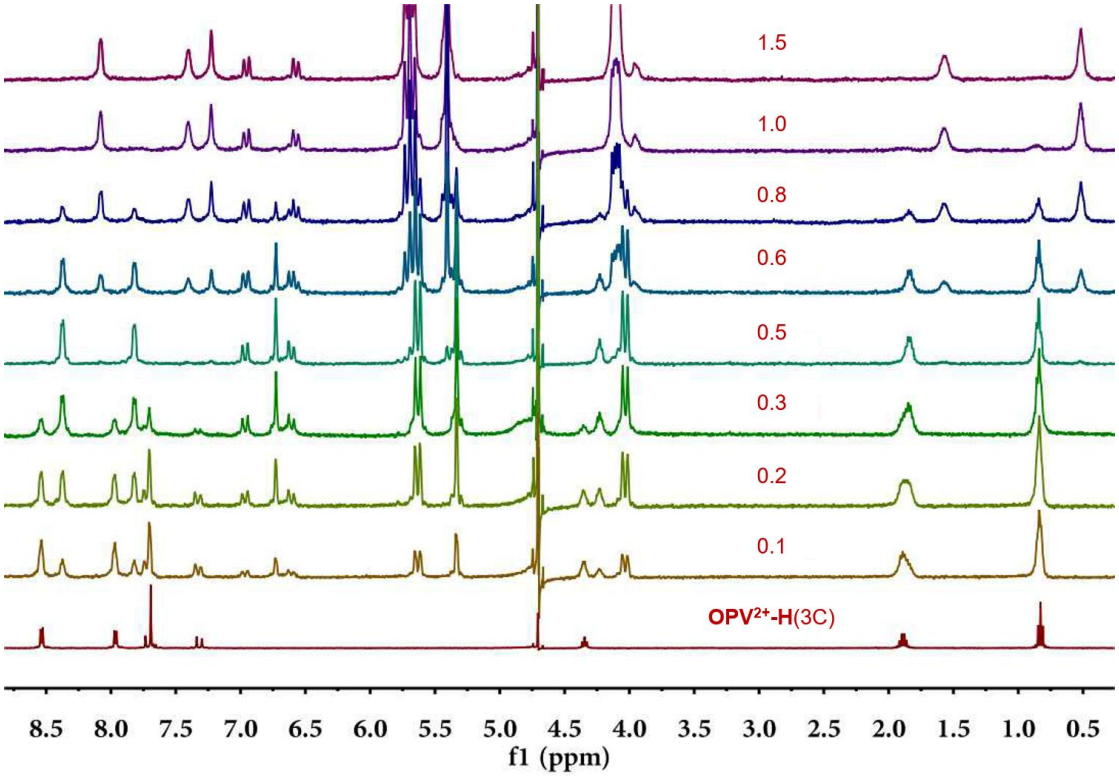

Fig. S4-3 ^{1}H NMR spectrum of **OPV^{2+}-H** (3C) (1.0 mM in D_2O) with different concentration of Q[8] (0.1-1.5 eq.).

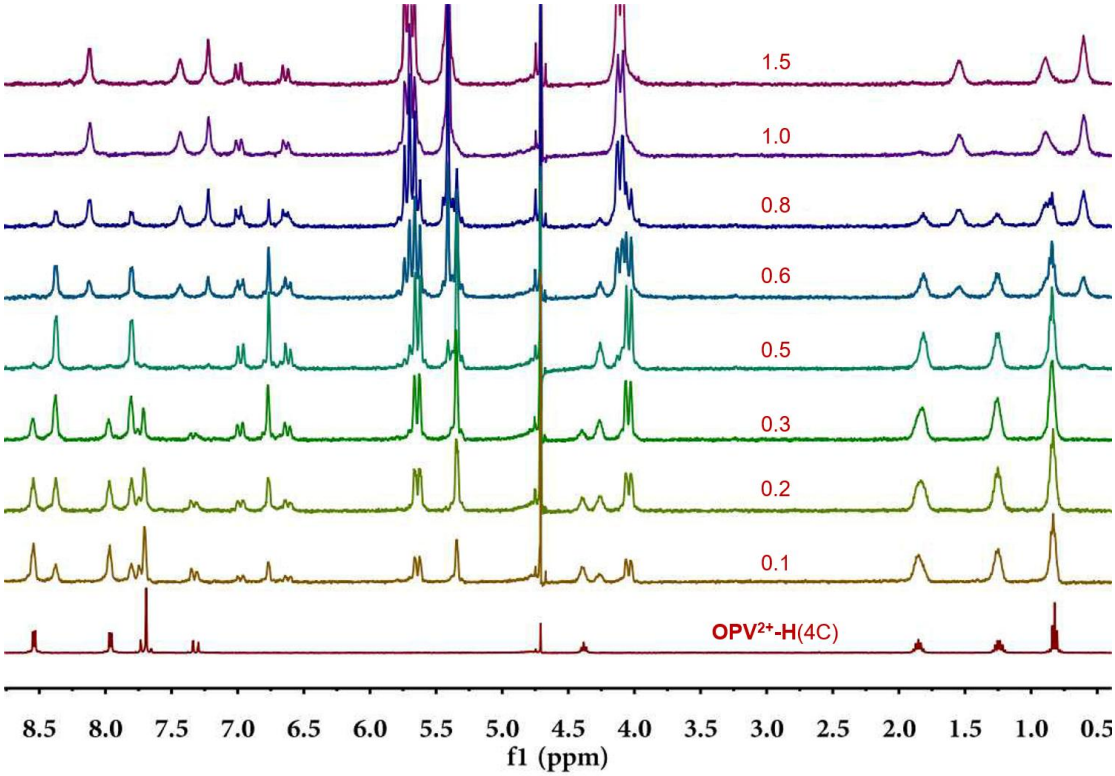

Fig. S4-4 ^{1}H NMR spectrum of **OPV^{2+}-H** (4C) (1.0 mM in D_2O) with different concentration of Q[8] (0.1-1.5 eq.).

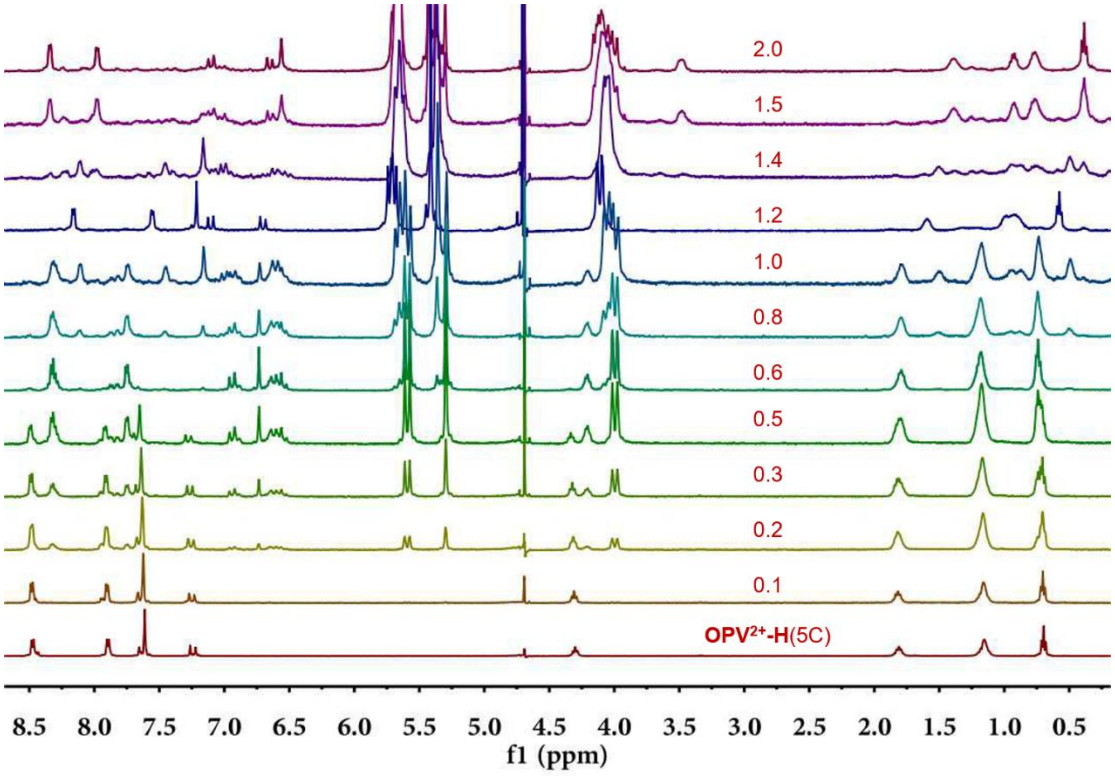

Fig. S4-5 ^{1}H NMR spectrum of **OPV^{2+}-H** (5C) (1.0 mM in D_2O) with different concentration of Q[8] (0.1~2.0 eq.).

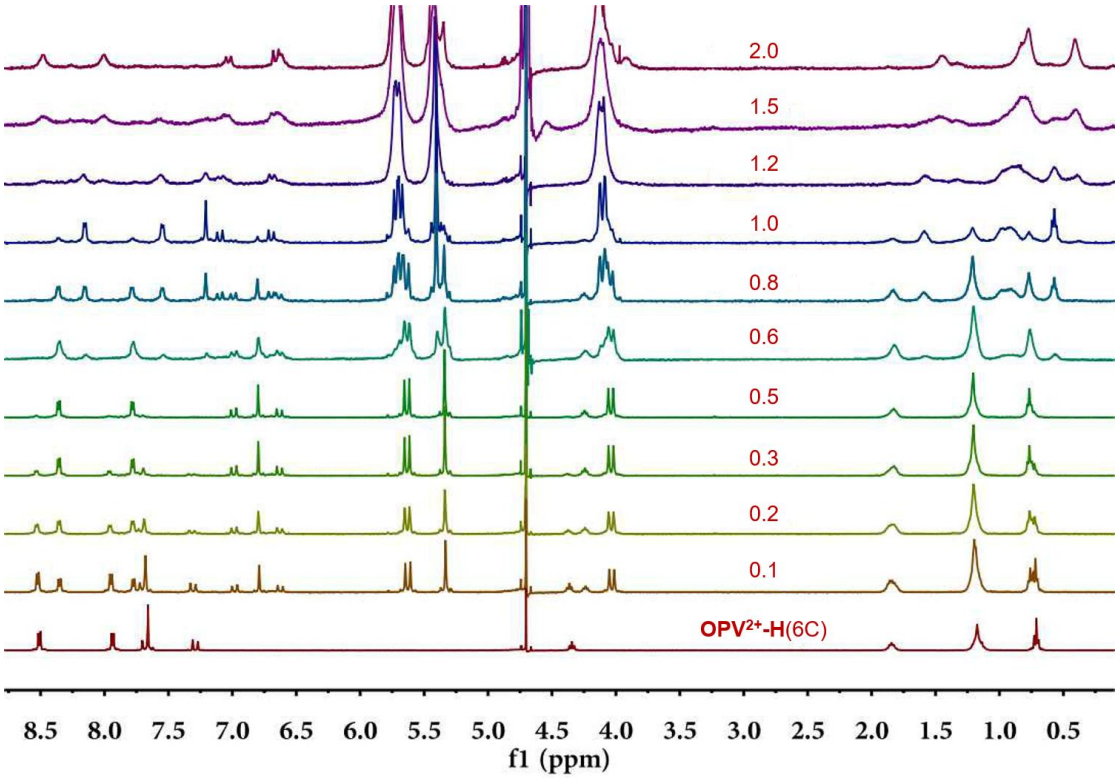

Fig. S4-6 ^{1}H NMR spectrum of **OPV^{2+}-H** (6C) (1.0 mM in D_2O) with different concentration of Q[8] (0.1~2.0 eq.).

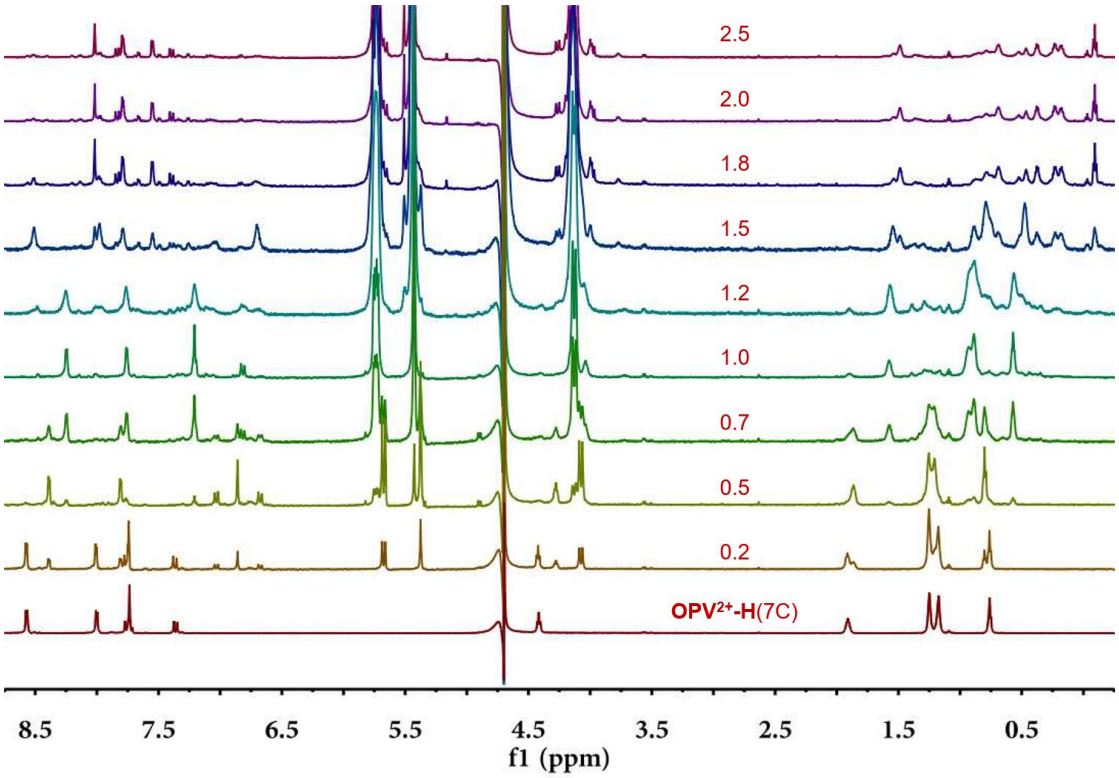

Fig. S4-7 ^{1}H NMR spectrum of **OPV^{2+}-H** (7C) (0.7 mM in D_2O) with different concentration of Q[8] (0.2~2.5 eq.).

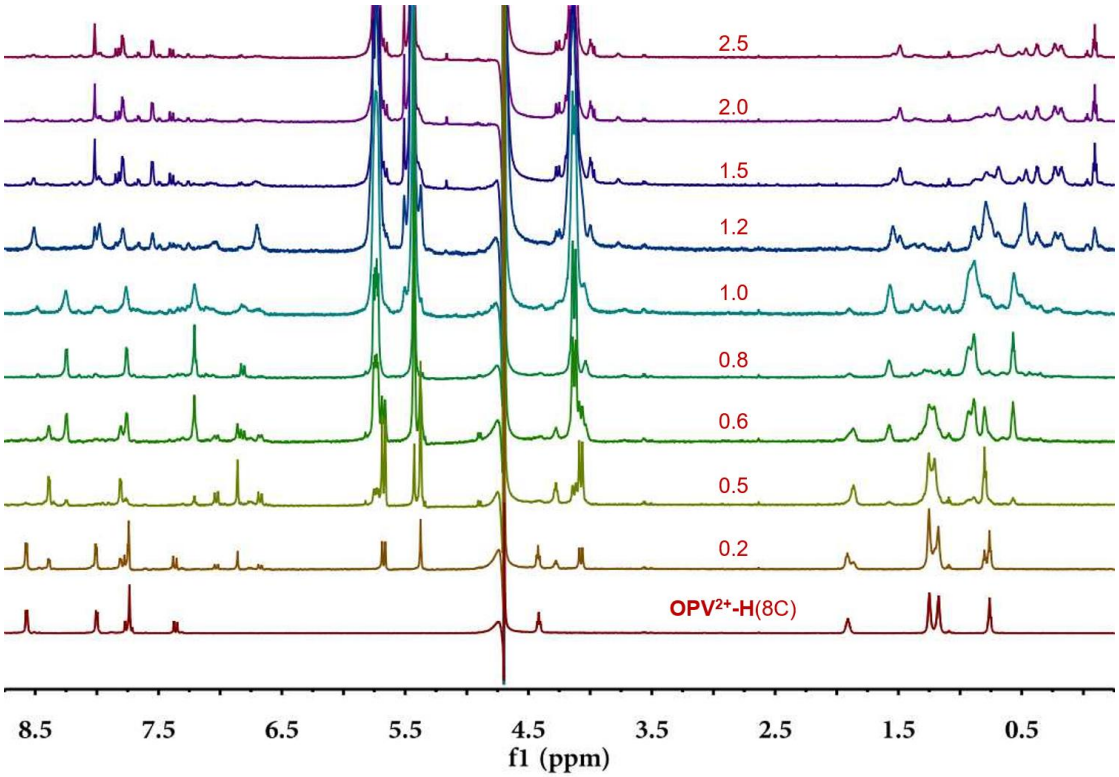

Fig. S4-8 ^{1}H NMR spectrum of **OPV^{2+}-H** (8C) (0.7 mM in D_2O) with different concentration of Q[8] (0.2~2.5 eq.).

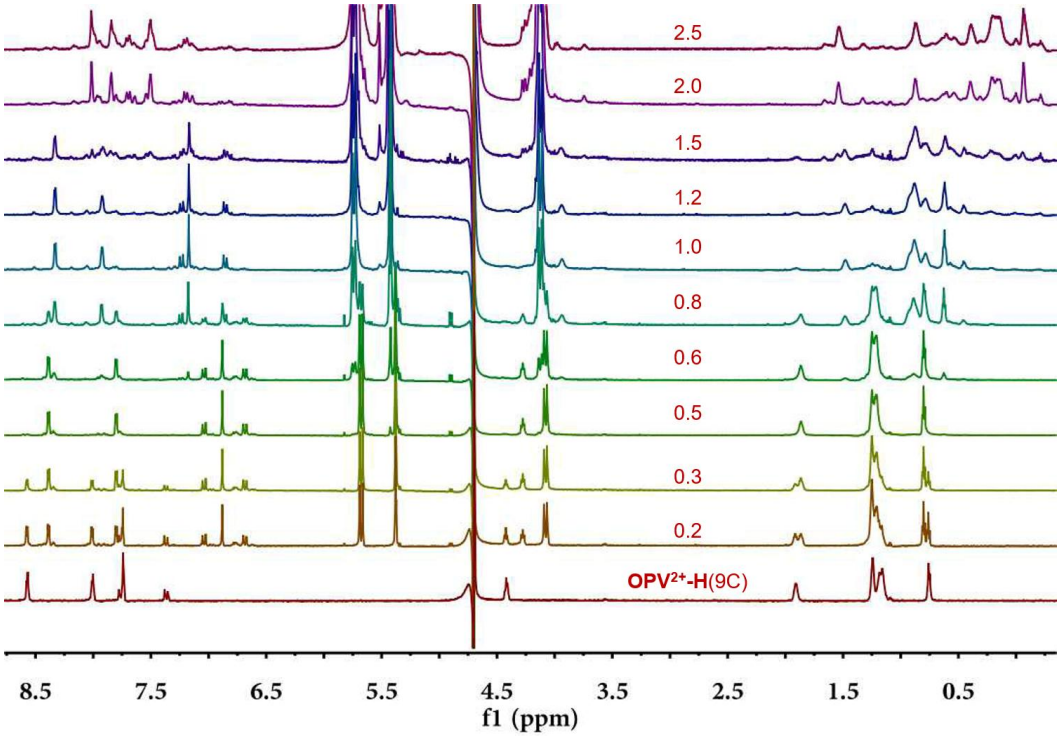

Fig. S4-9 ^{1}H NMR spectrum of **OPV^{2+}-H** (9C) (0.7 mM in D_2O) with different concentration of Q[8] (0.2~2.5 eq.).

Fig. S5 ^{1}H NMR spectrum of **OPV^{2+}-Me** (1C-9C) with different concentration of Q[8].

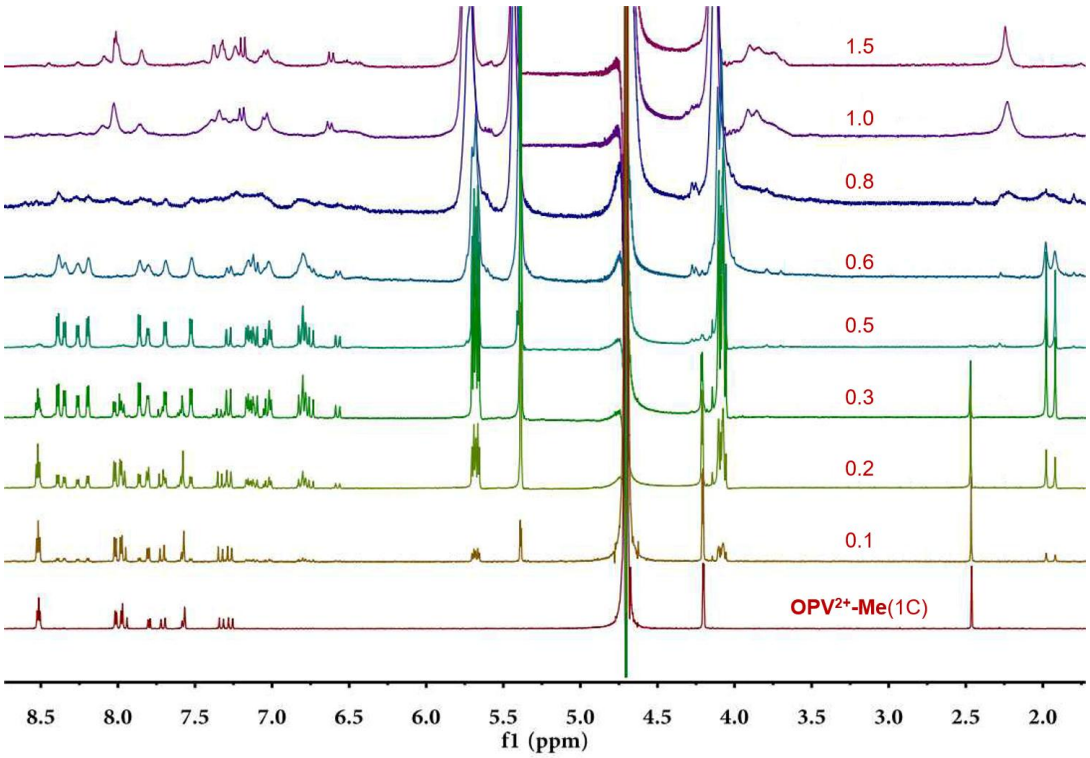

Fig. S5-1 ^{1}H NMR spectrum of **OPV^{2+}-Me** (1C) (1.0 mM in D_2O) with different concentration of Q[8] (0.1~1.5 eq.).

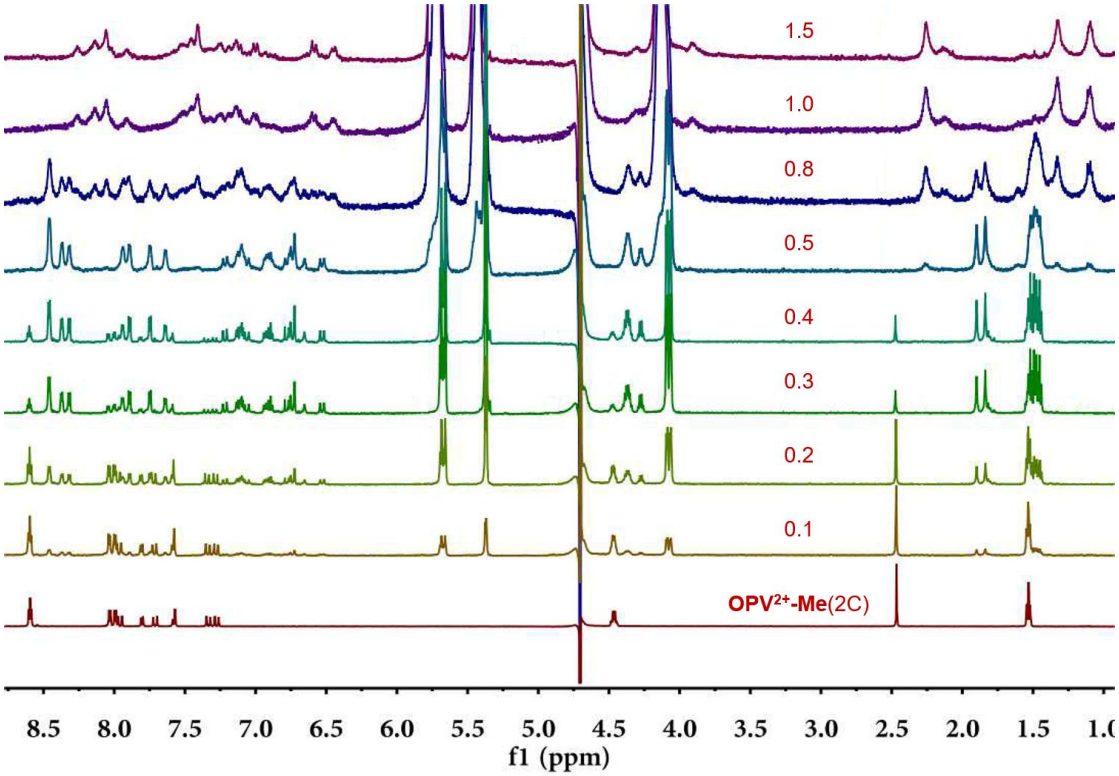

Fig. S5-2 ^{1}H NMR spectrum of **OPV^{2+}-Me** (2C) (1.0 mM in D_2O) with different concentration of Q[8] (0.1~1.5 eq.).

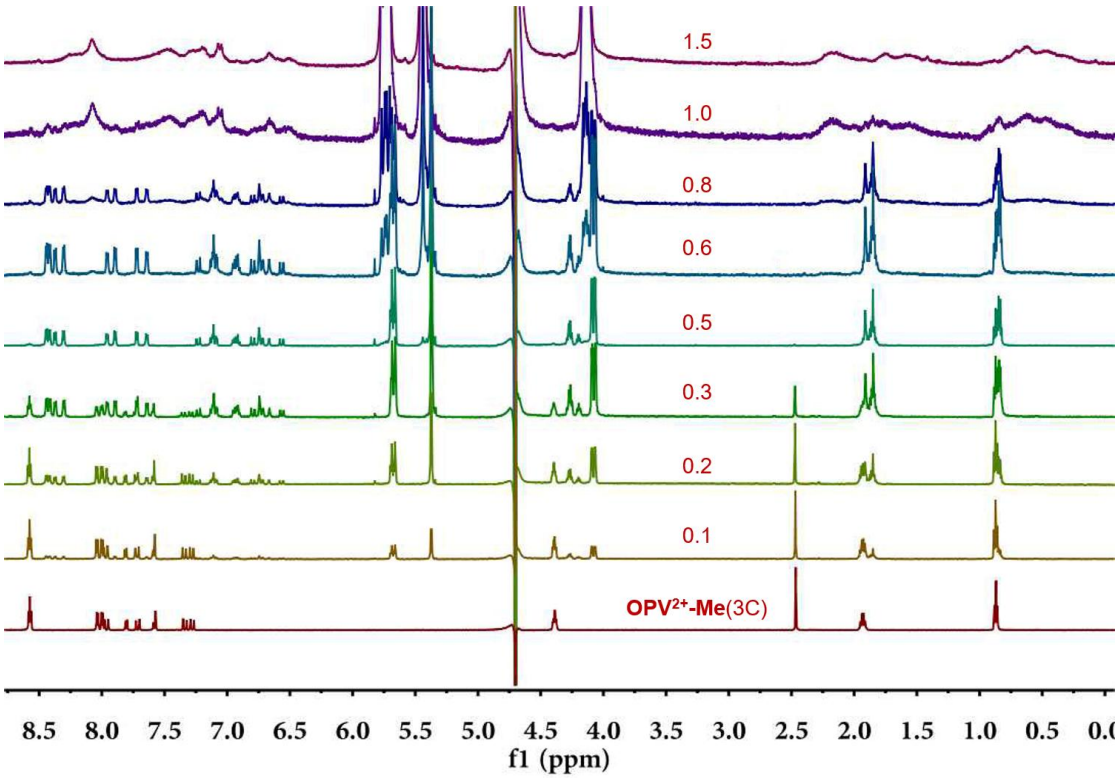

Fig. S5-3 ^{1}H NMR spectrum of **OPV^{2+}-Me** (3C) (1.0 mM in D_2O) with different concentration of Q[8] (0.1~1.5 eq.).

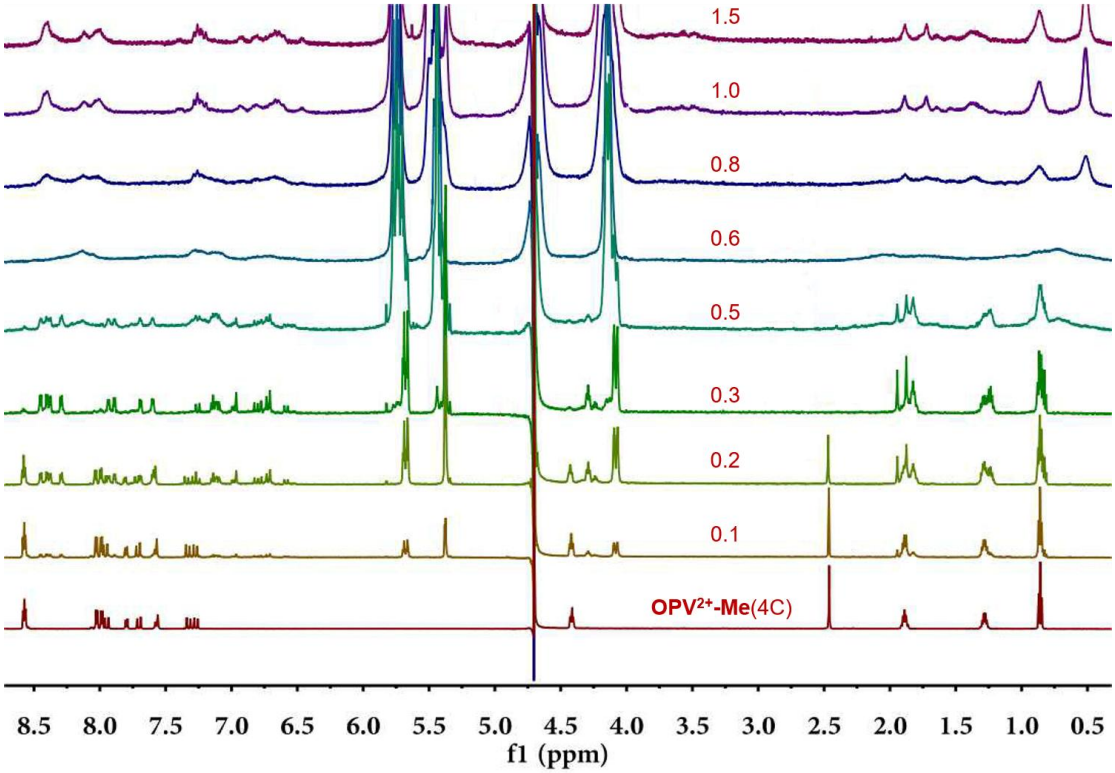

Fig. S5-4 ^{1}H NMR spectrum of **OPV^{2+}-Me** (4C) (1.0 mM in D_2O) with different concentration of Q[8] (0.1~1.5 eq.).

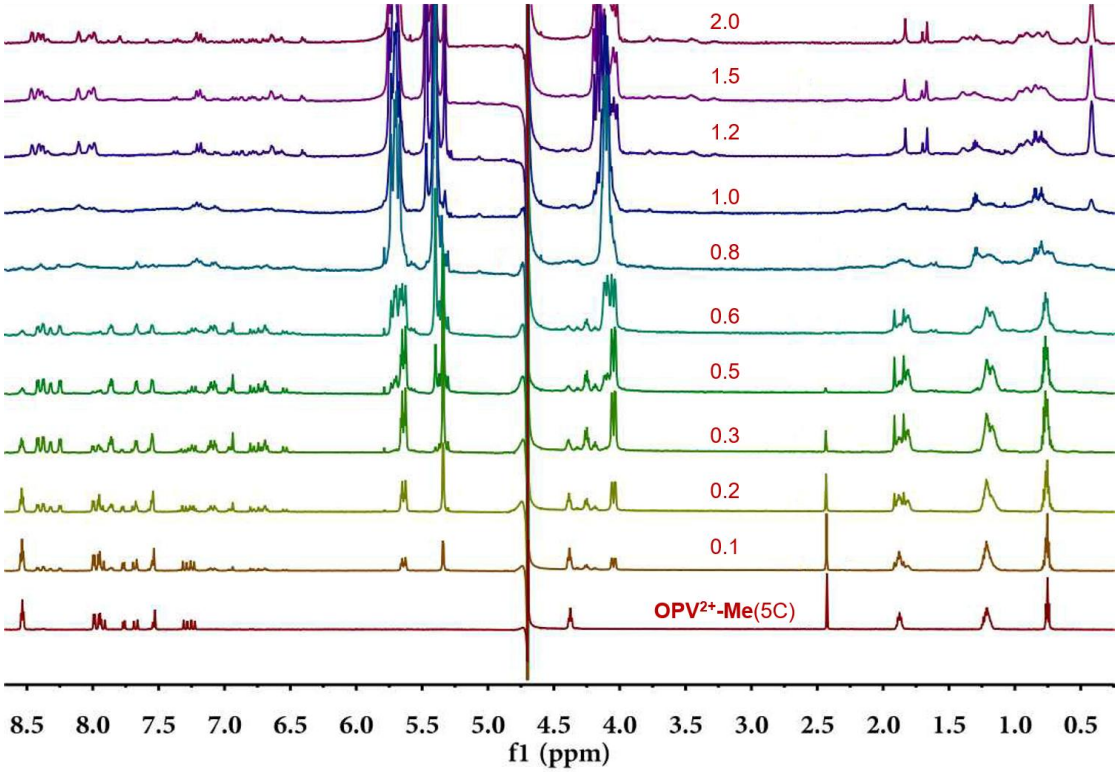

Fig. S5-5 ^{1}H NMR spectrum of **OPV^{2+}-Me** (5C) (0.7 mM in D_2O) with different concentration of Q[8] (0.1~2.0 eq.).

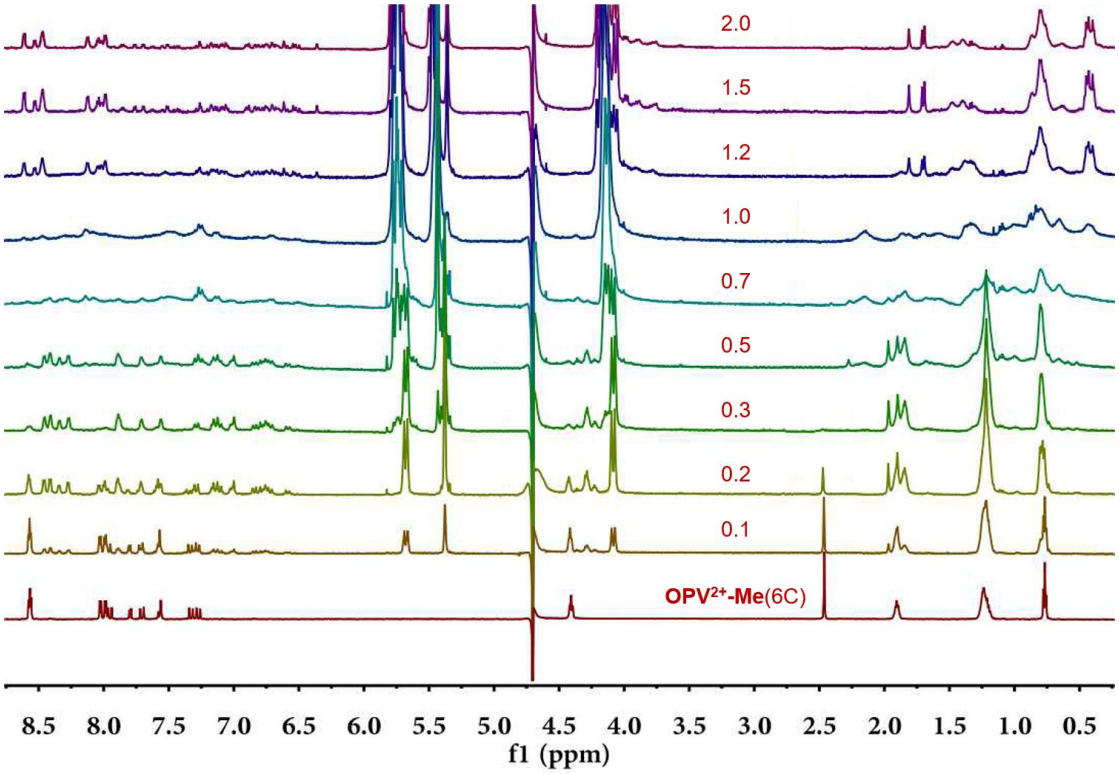

Fig. S5-6 ^{1}H NMR spectrum of **OPV^{2+}-Me** (6C) (0.7 mM in D_2O) with different concentration of Q[8] (0.1~2.0 eq.).

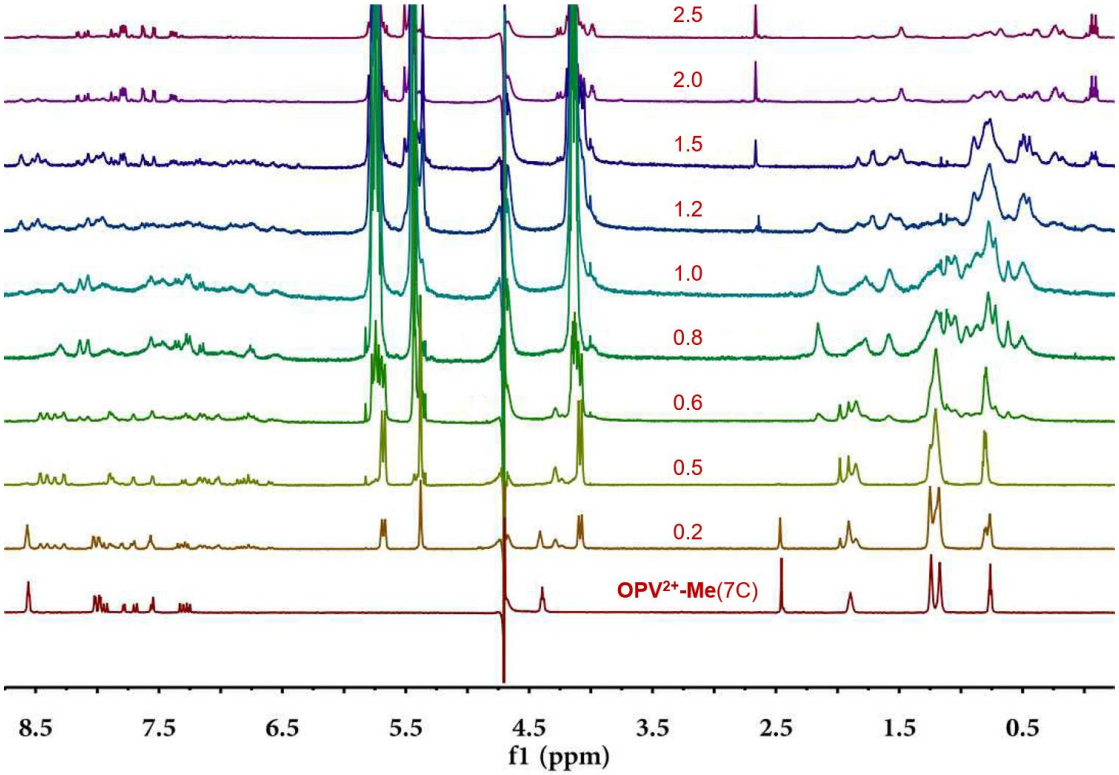

Fig. S5-7 ^{1}H NMR spectrum of **OPV^{2+}-Me** (7C) (0.6 mM in D_2O) with different concentration of Q[8] (0.2~2.5 eq.).

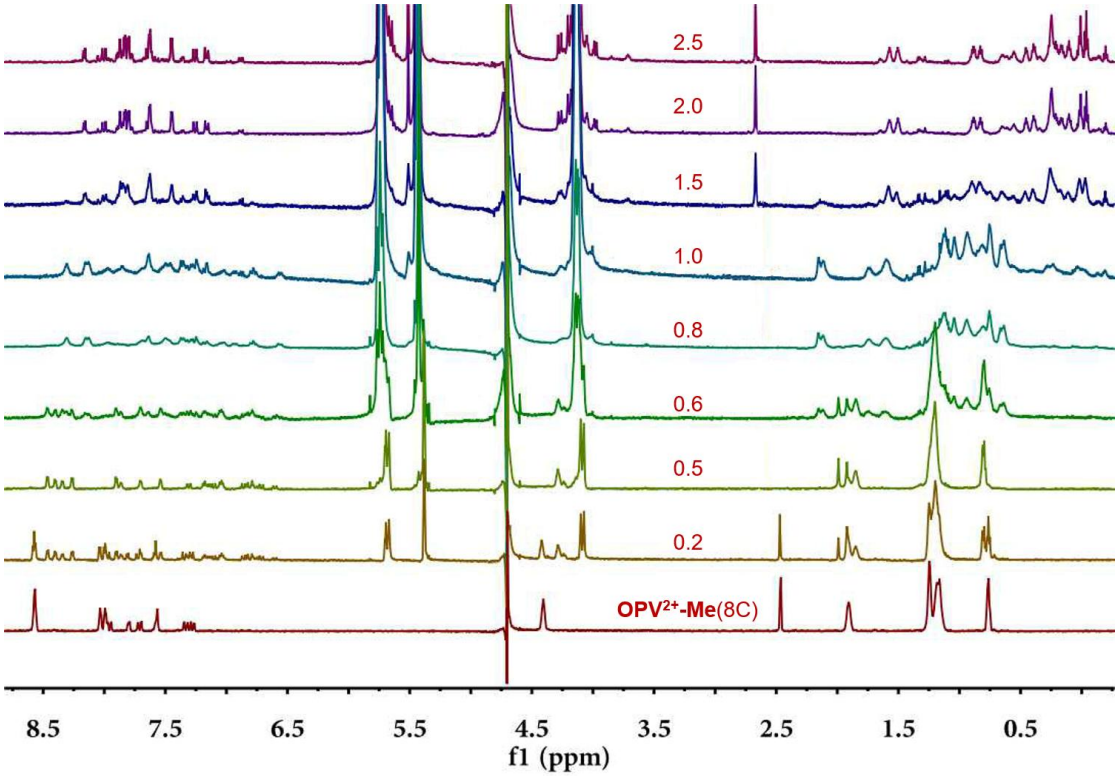

Fig. S5-8 ^{1}H NMR spectrum of **OPV^{2+}-Me** (8C) (0.6 mM in D_2O) with different concentration of Q[8] (0.2~2.5 eq.).

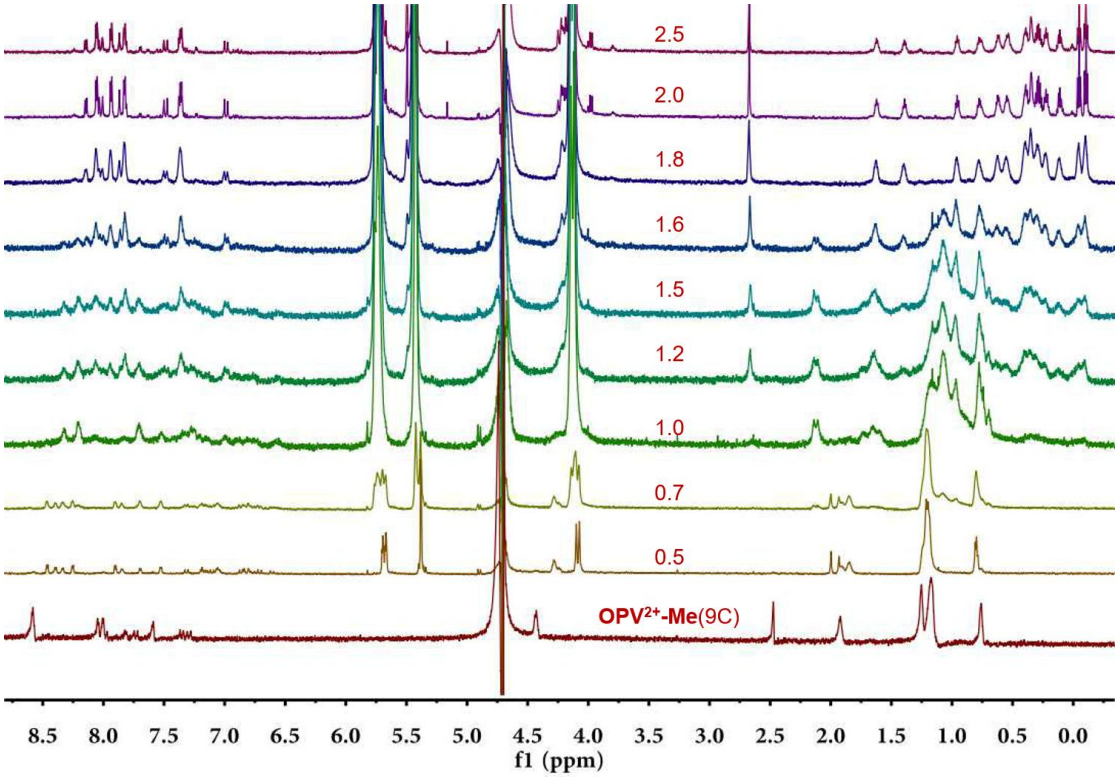

Fig. S5-9 ^{1}H NMR spectrum of **OPV^{2+}-Me** (9C) (0.6 mM in D_2O) with different concentration of Q[8] (0.5~2.5 eq.).

Fig. S6 ^{1}H NMR spectrum of **OPV^{2+}-2Me** (1C-9C) with different concentration of Q[8].

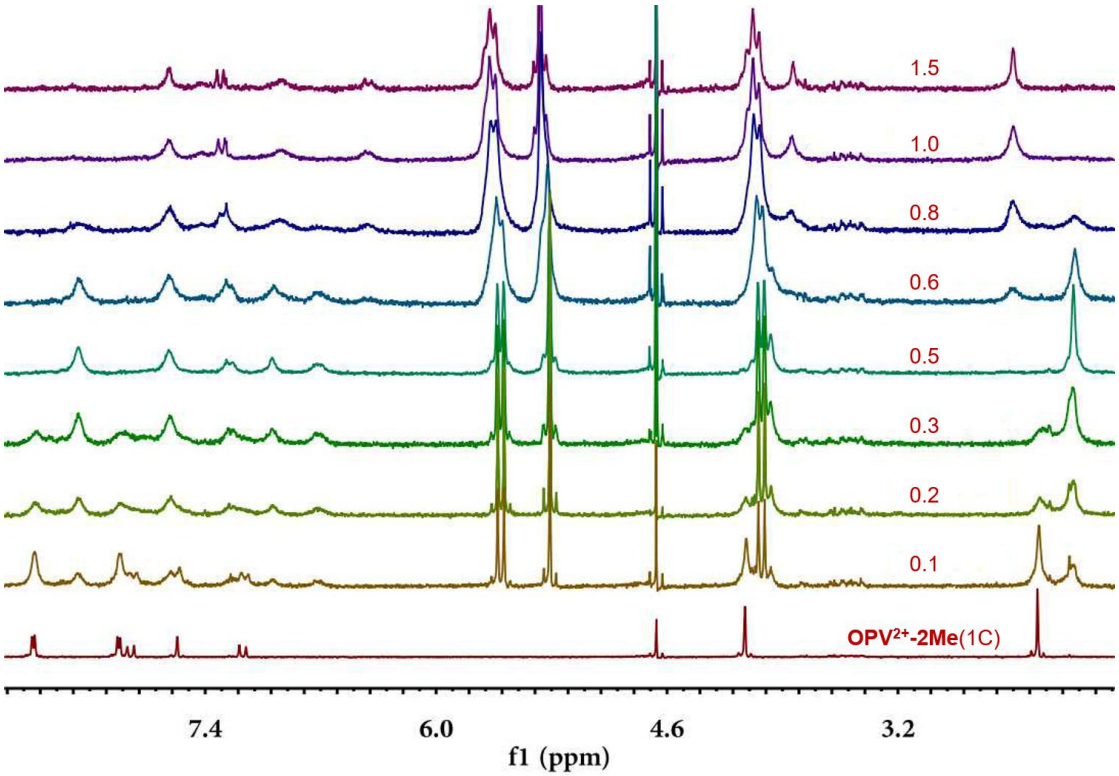

Fig. S6-1 ^{1}H NMR spectrum of **OPV^{2+}-2Me** (1C) (1.0 mM in D_2O) with different concentration of Q[8] (0.1~1.5 eq.).

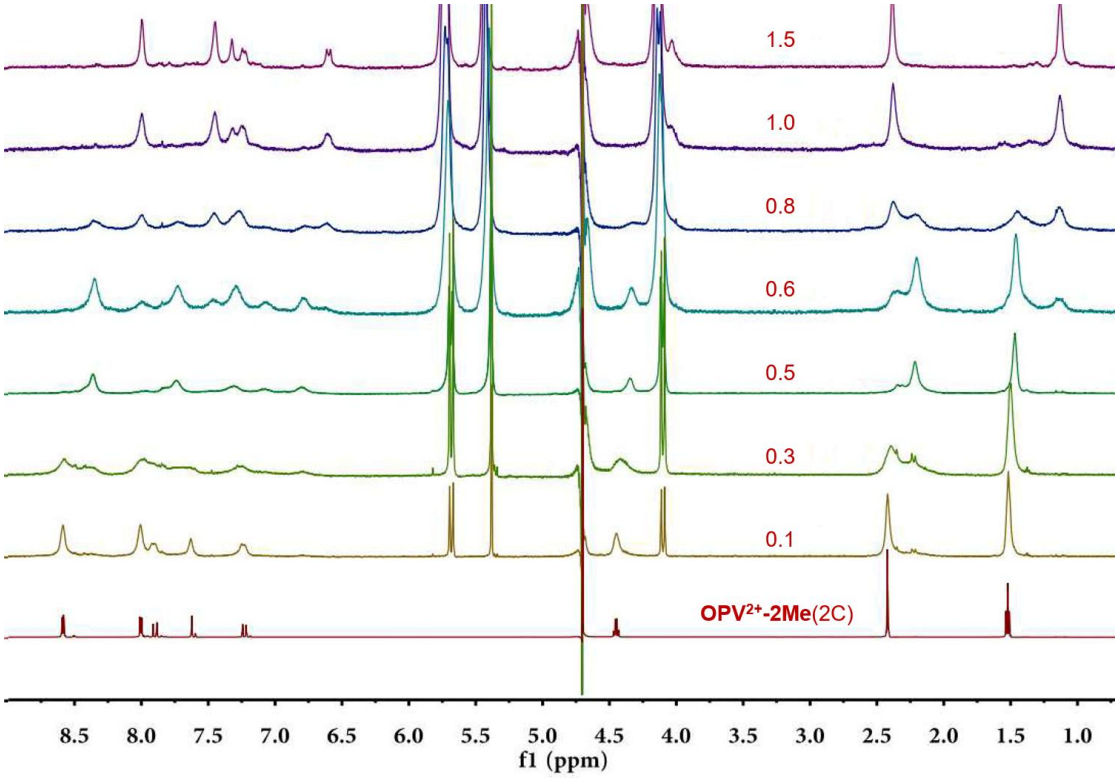

Fig. S6-2 ^{1}H NMR spectrum of **OPV^{2+}-2Me** (2C) (1.0 mM in D_2O) with different concentration of Q[8] (0.1~1.5 eq.).

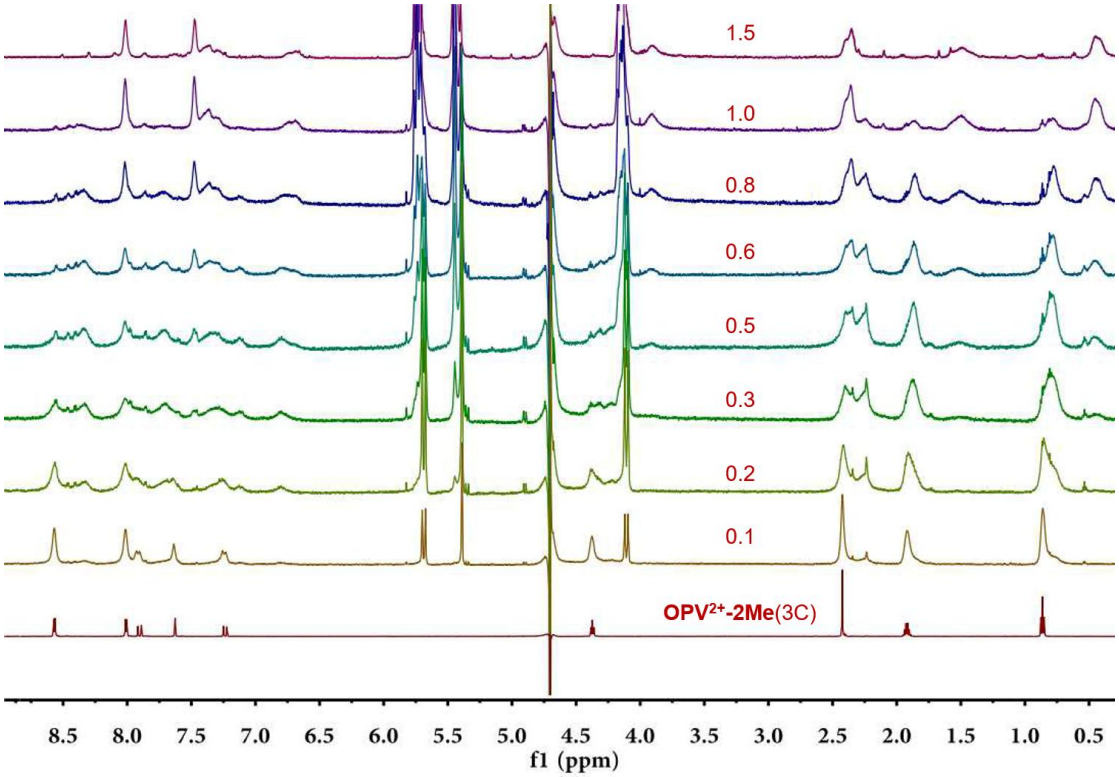

Fig. S6-3 ^{1}H NMR spectrum of **OPV^{2+}-2Me** (3C) (1.0 mM in D_2O) with different concentration of Q[8] (0.1~1.5 eq.).

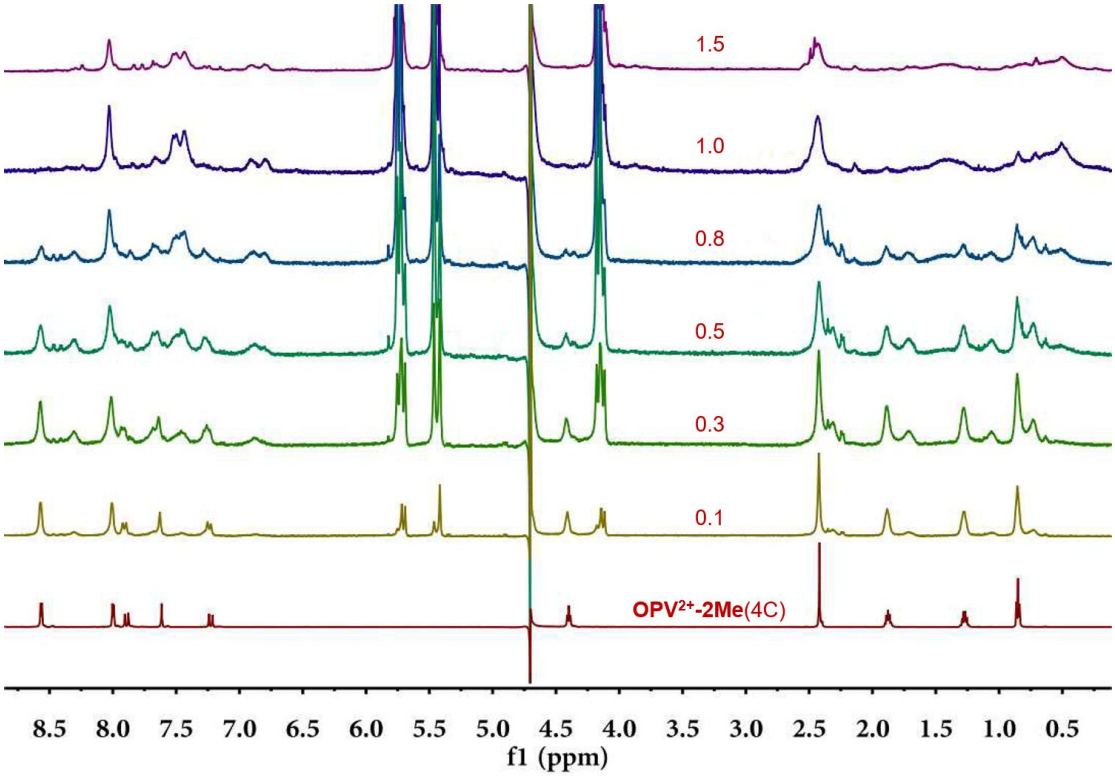

Fig. S6-4 ^{1}H NMR spectrum of **OPV^{2+}-2Me** (4C) (1.0 mM in D_2O) with different concentration of Q[8] (0.1~1.5 eq.).

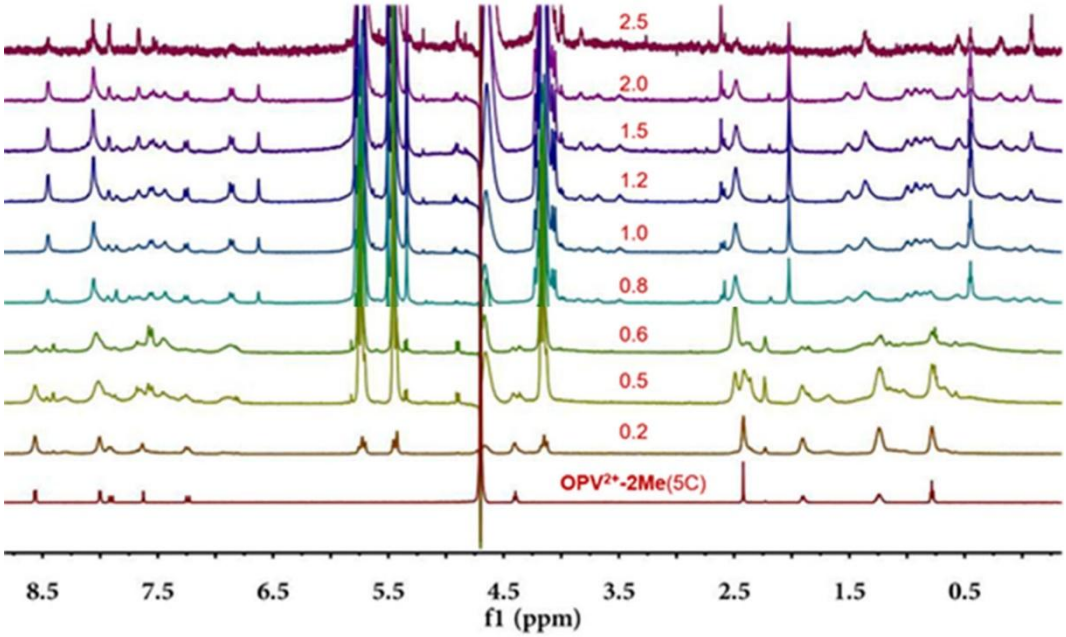

Fig. S6-5 ^{1}H NMR spectrum of **OPV^{2+}-2Me** (5C) (0.6 mM in D_2O) with different concentration of Q[8] (0.2~2.5 eq.).

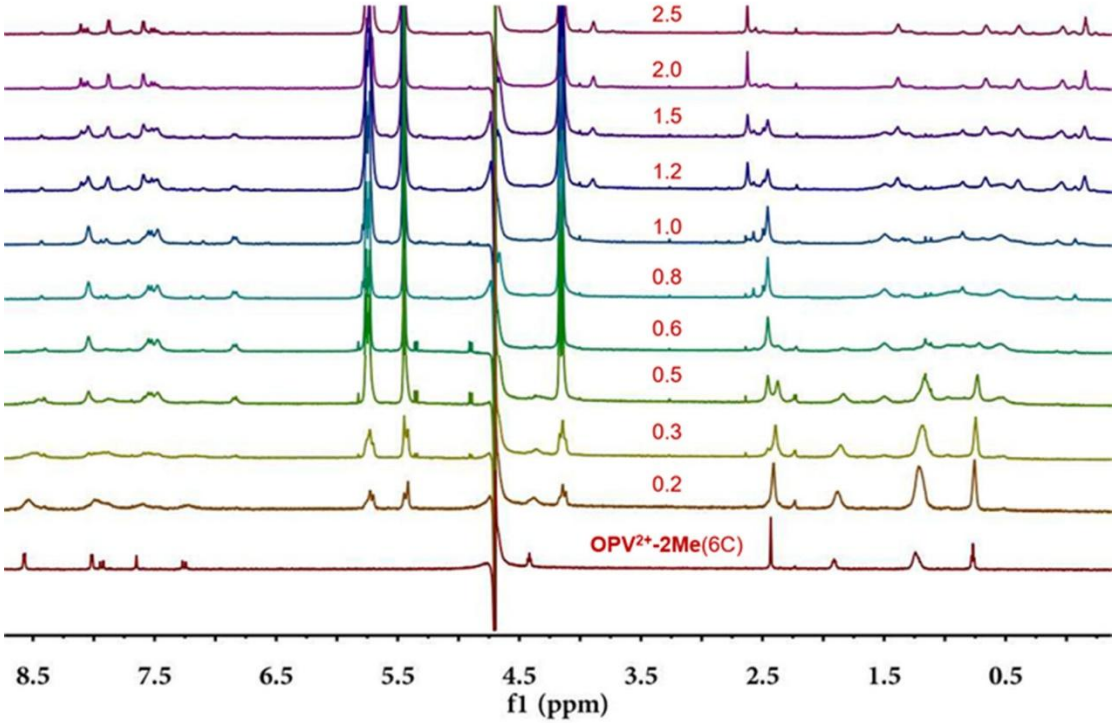

Fig. S6-6 ^{1}H NMR spectrum of **OPV^{2+}-2Me** (6C) (0.6 mM in D_2O) with different concentration of Q[8] (0.2~2.5 eq.).

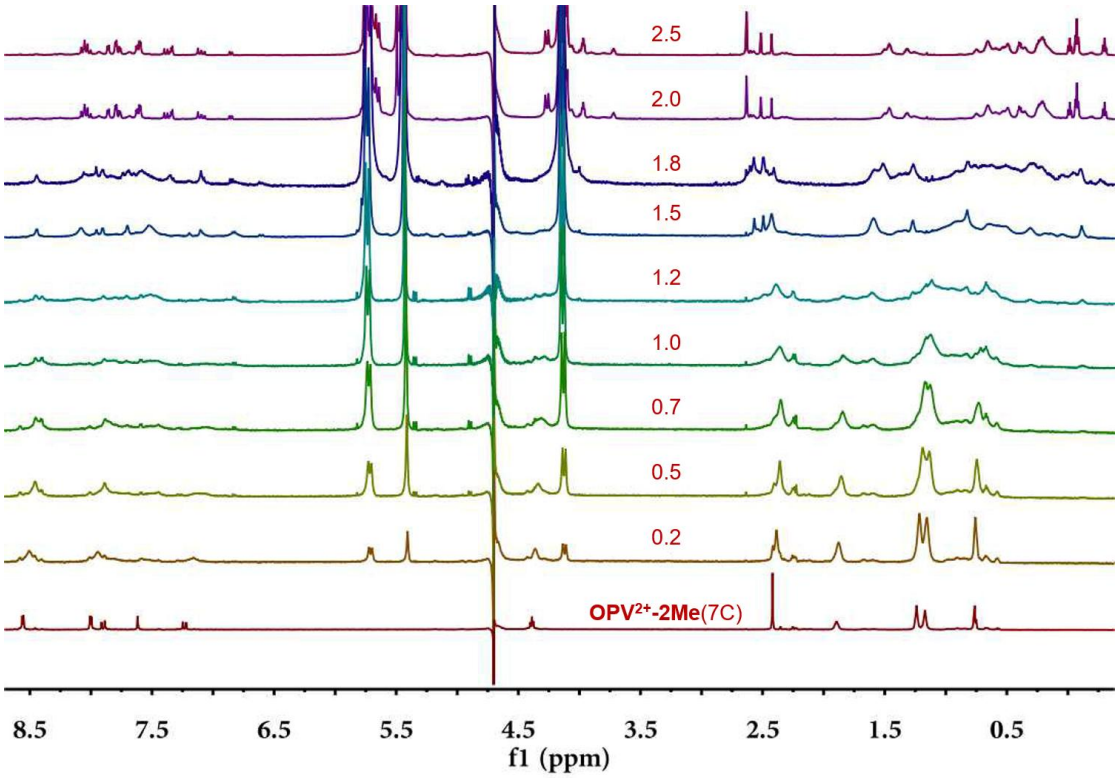

Fig. S6-7 ^{1}H NMR spectrum of **OPV^{2+}-2Me** (7C) (0.6 mM in D_2O) with different concentration of Q[8] (0.2~2.5 eq.).

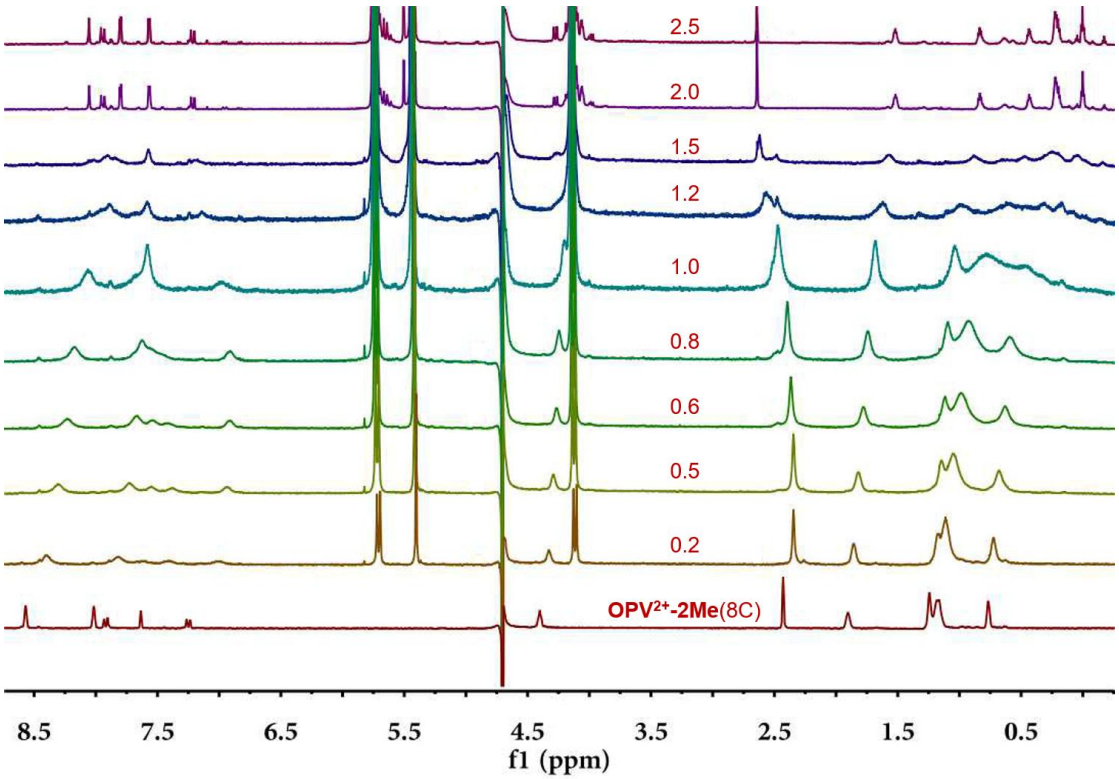

Fig. S6-8 ^{1}H NMR spectrum of **OPV^{2+}-2Me** (8C) (0.6 mM in D_2O) with different concentration of Q[8] (0.2~2.5 eq.).

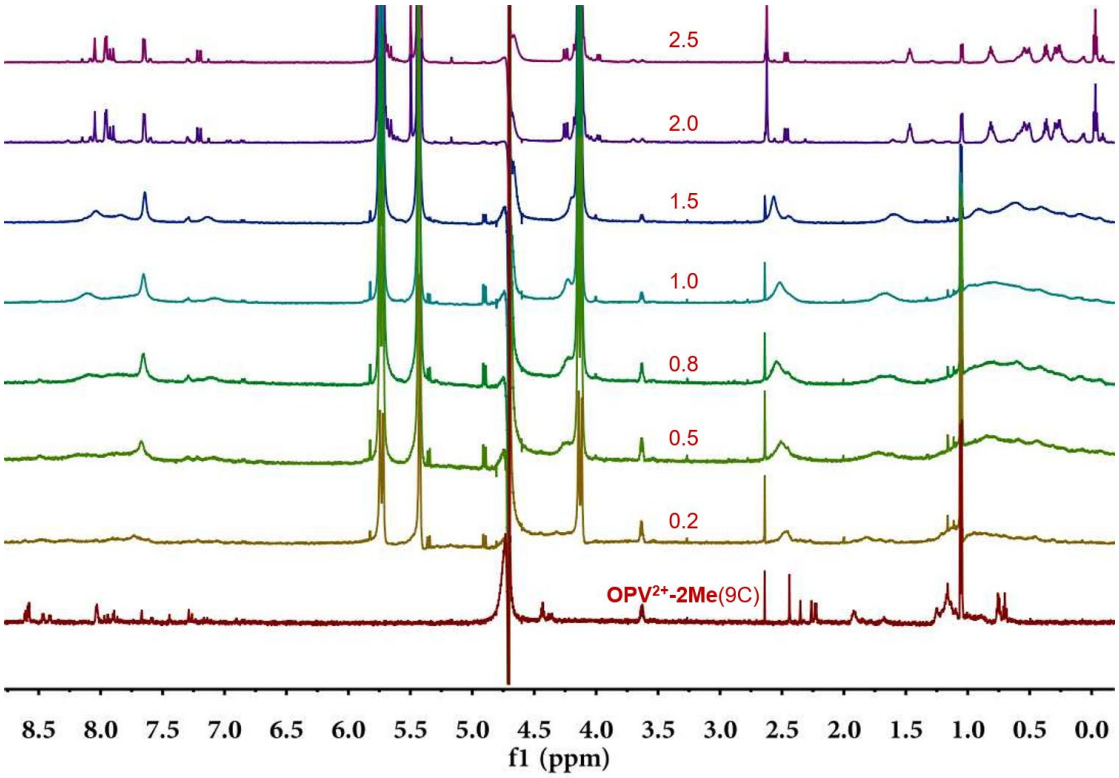

Fig. S6-9 ^{1}H NMR spectrum of **OPV^{2+}-2Me** (9C) (0.5 mM in D_2O) with different concentration of Q[8] (0.2~2.5 eq.).

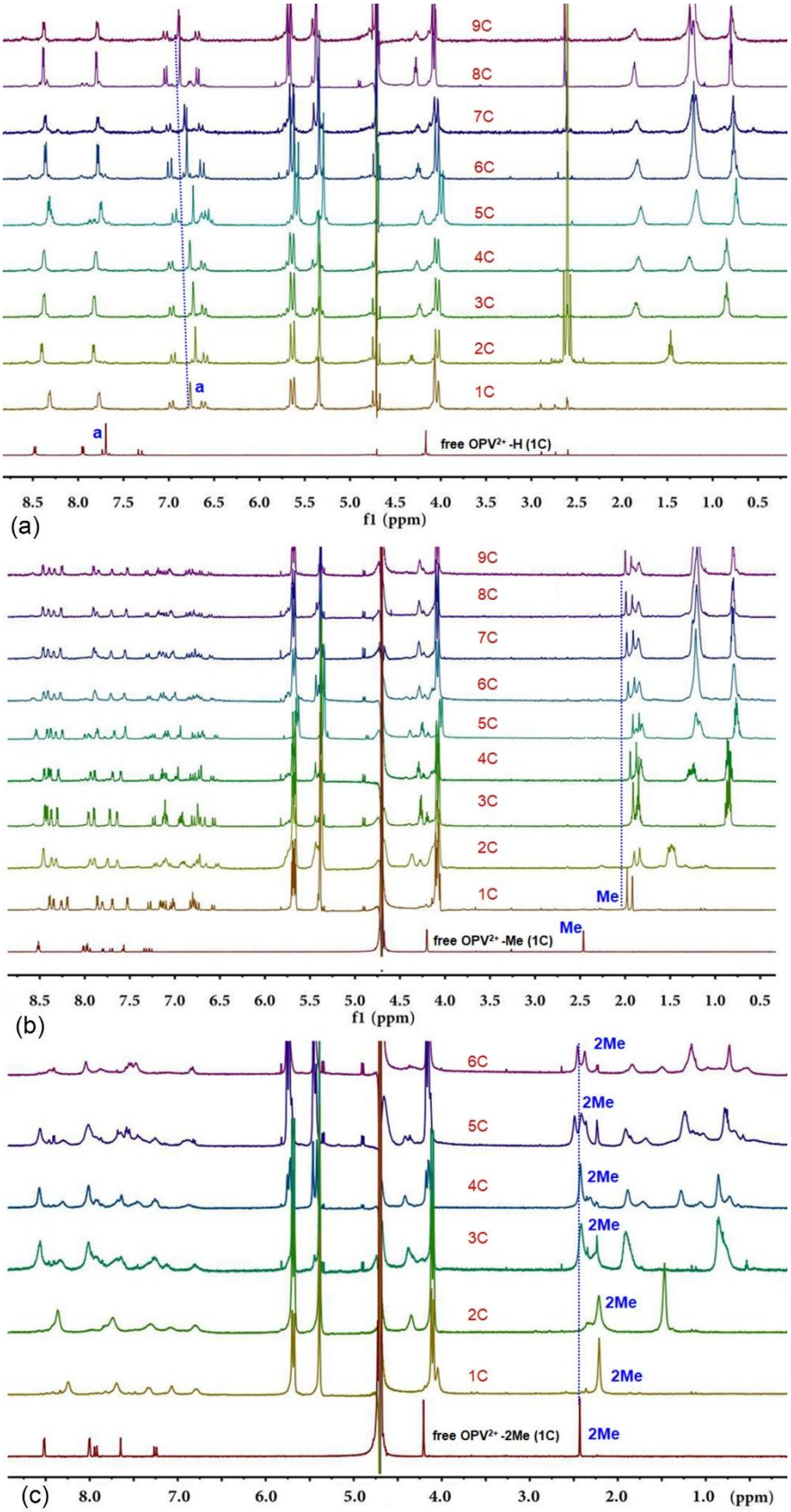

Fig. S7 ^{1}H NMR spectra of (a) **OPV^{2+}-H** (1C-9C); (b) **OPV^{2+}-Me** (1C-9C); (c) **OPV^{2+}-2Me**(1C-6C) in the presence of 0.5 eq. of Q[8].

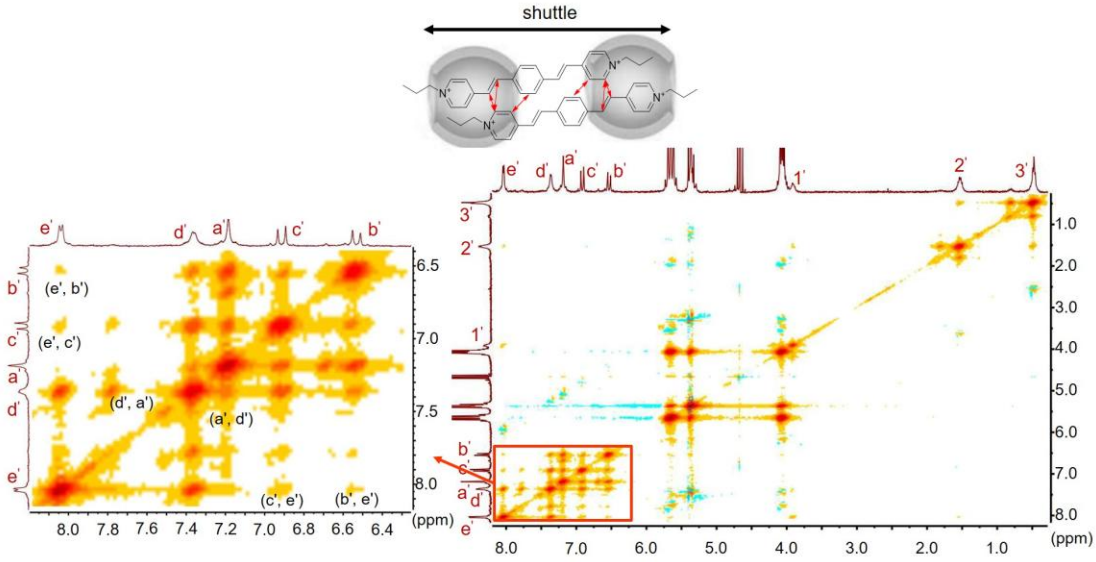

Fig. S8 ^{1}H-^{1}H NOESY of **OPV^{2+}-H** (3C)/Q[8] with a molar ratio of 2:2.

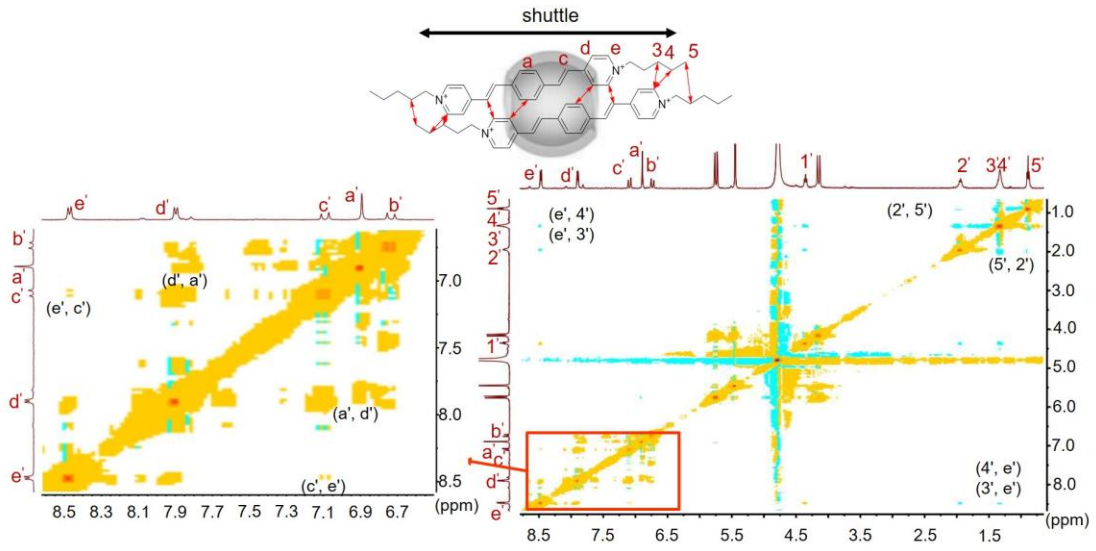

Fig. S9 ^{1}H-^{1}H NOESY of **OPV^{2+}-H** (5C)/Q[8] with a molar ratio of 2:1.

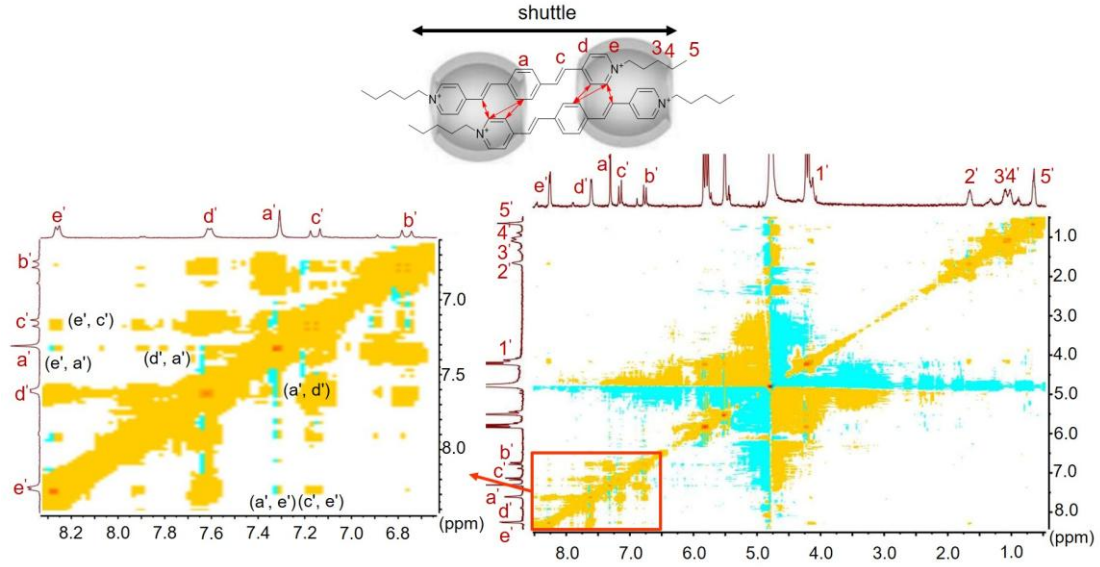

Fig. S10 ^{1}H-^{1}H NOESY of **OPV^{2+}-H** (5C)/Q[8] with a molar ratio of 2:2

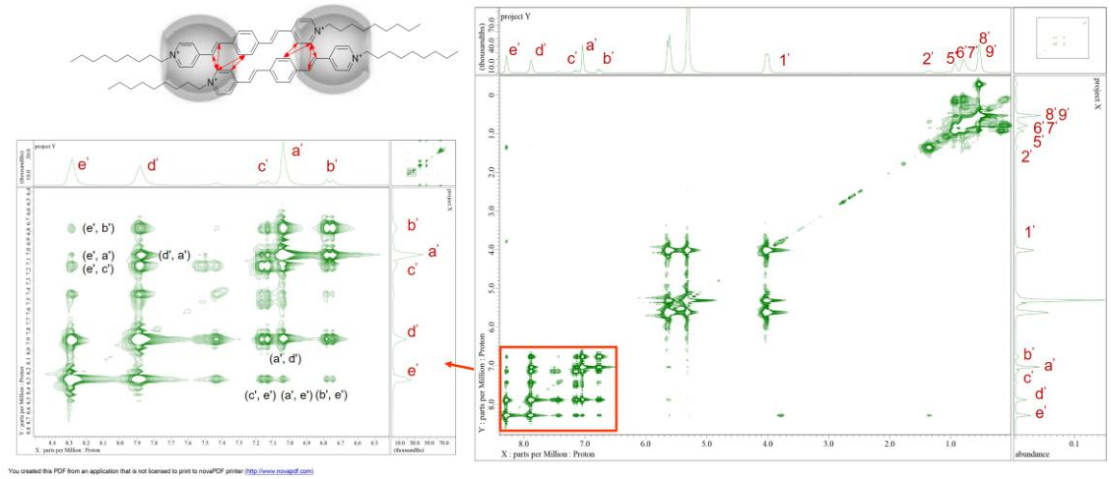

Fig. S11 ^{1}H-^{1}H NOESY of **OPV^{2+}-H** (9C)/Q[8] with a molar ratio of 2:2

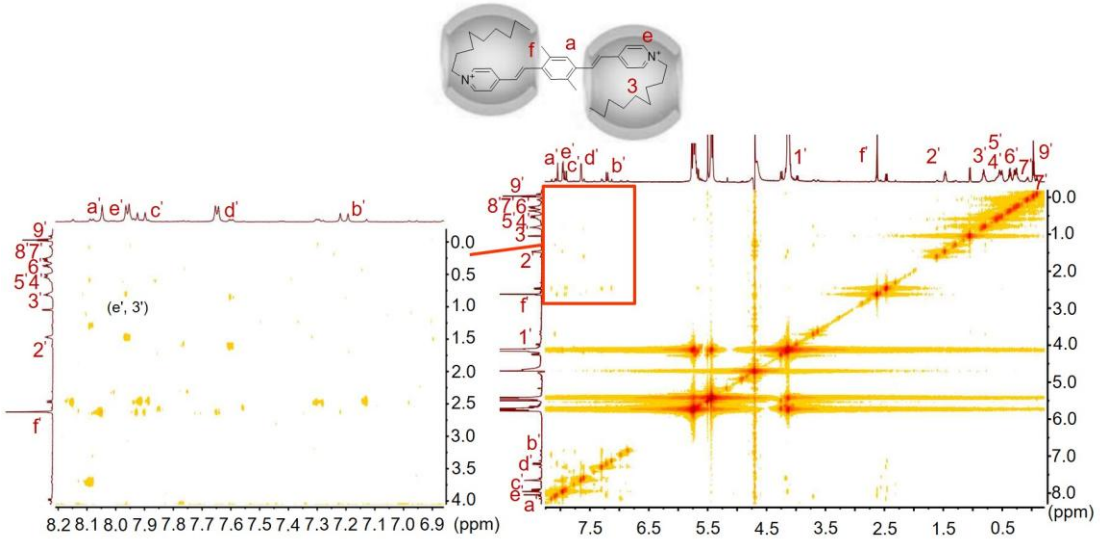

Fig. S12 ^{1}H-^{1}H NOESY of **OPV^{2+}-2Me** (9C)/Q[8] with a molar ratio of 1:2

Fluorescence lifetime measurements: Fluorescence lifetime measurements were obtained using the time-correlated single photon counting (TCSPC) method with an Edinburgh Instrument FLS 980 fluorospectrometer at 25 ^{o}C. The excitation source was a 375 nm EPLED Laser. And a microchannel plate photomultiplier tube (R928P-PMT) was used for fluorescence detection. Decay time data analysis was made with the method of nonlinear last square iterative reconvolution. The quality of the fit was estimated by the reduced chi-square χ^2 and the autocorrelation function of the residuals. The consequences are shown in the Table S2.

Table S2. Average fluorescence lifetime (τ, ns) in the presence of Q[8] (0, 0.5, 1.0, 1.5, or 2.0 eq.)

Sample	Free	0.5 eq.	1.0 eq.	1.5 eq.	2.0 eq.
OPV^{2+}-H（1C）	0.13	11.22	11.81		
OPV^{2+}-H（2C）	0.12	14.89	9.26		
OPV^{2+}-H（3C）	0.12	11.28	8.65		
OPV^{2+}-H（4C）	0.12	9.41	8.70		
OPV^{2+}-H（5C）	0.13	10.97	9.85	15.93	
OPV^{2+}-H（6C）	0.14	12.30	9.22	15.91	
OPV^{2+}-H（7C）	0.15	8.67	7.69		0.68
OPV^{2+}-H（8C）	0.18	7.90	6.83		1.07
OPV^{2+}-H（9C）	0.16	6.71	6.52		1.15
OPV^{2+}-Me（1C）	0.11	12.75	10.12		
OPV^{2+}-Me（2C）	0.12	10.68	10.97		
OPV^{2+}-Me（3C）	0.10	10.61	9.58		
OPV^{2+}-Me（4C）	0.12	10.37	9.83		
OPV^{2+}-Me（5C）	0.12	10.67	10.93	14.69	
OPV^{2+}-Me（6C）	0.15	10.95	10.81	11.53	
OPV^{2+}-Me（7C）	0.15	11.48	10.81		0.75
OPV^{2+}-Me（8C）	0.13	12.90	9.85		0.49
OPV^{2+}-Me（9C）	0.10	13.05	6.58		0.61
OPV^{2+}-2Me（1C）	0.11	13.99	10.61		
OPV^{2+}-2Me（2C）	0.11	11.07	9.80		
OPV^{2+}-2Me（3C）	0.12	9.00	9.19		
OPV^{2+}-2Me（4C）	0.12	10.72	9.28		
OPV^{2+}-2Me（5C）	0.14	12.62	10.50		0.55
OPV^{2+}-2Me（6C）	0.14	11.18	10.29		0.29
OPV^{2+}-2Me（7C）	0.13	0.19	0.27		0.31
OPV^{2+}-2Me（8C）	0.13	0.17	0.23		0.40
OPV^{2+}-2Me（9C）	0.13	0.18	0.26		0.40

Absolute emission quantum yield measurements: Emission quantum yield (Φ) measurements were carried out using Edinburgh instrument model FLS980 equipped with 450W Xenon arc lamp at 25 ^{o}C. Quantum yield of the samples (Table S3) were calculated based on the absolute method using integrating sphere of diameter 15 cm coated with tetrafluoroethylene after standardization. The performance of the integrating sphere was verified by using rhodamine B as test sample. The absolute quantum yield was calculated for rhodamine B first and compared with its literature value (0.21) in water, which matched very well. It was assumed that light falling to tetrafluoroethylene coating are scattered perfectly (100%). Sample holder is kept in the centre of sphere and scattered light was collected by detector through two windows: one for entrance of exciting light and another for collection of scattered/emitted light.

Emission quantum yield (Φ) is related to number of photons absorbed (α) and number of photons emitted by the sample (ε) as

$$\Phi = \frac{\varepsilon}{\alpha} = \frac{\int I_{Emission}}{\int I_{Solvent} - \int I_{Sample}}$$

where, $I_{emission}$ is emission spectrum of sample, $I_{solvent}$ is the spectrum of light used to excite only solvent (water) and I_{sample} is the spectrum of light used for exciting sample in solvent.

Table S3 Absolute emission quantum yield (QY/%)

Sample	Free	0.5 eq. Q[8]	1.0 eq. Q[8]	1.5 eq. Q[8]	2.0 eq. Q[8]
OPV^{2+}-H (1C)	5.69	19.33	37.41		
OPV^{2+}-H (3C)	5.64	22.74	31.89		
OPV^{2+}-H (5C)	4.40	29.99	25.03	22.62	
OPV^{2+}-H (9C)	5.97	34.01	23.62		16.045
OPV^{2+}-Me (1C)	5.68	34.81	35.05		
OPV^{2+}-Me (3C)	5.43	38.89	40.69		
OPV^{2+}-Me (5C)	5.79	29.99	24.14	33.49	
OPV^{2+}-Me (9C)	6.58	22.14	14.95		12.185
OPV^{2+}-2Me (1C)	5.52	31.64	27.00		
OPV^{2+}-2Me (3C)	6.72	26.97	24.16		
OPV^{2+}-2Me (5C)	5.88	34.83	20.54		11.84
OPV^{2+}-2Me (9C)	6.22				12.17

ITC measurements: All microcalorimetric titrations were performed in aqueous solution at atmospheric pressure and 298.15 K in a thermostated and fully computer-operated isothermal calorimetry (TA, U.S.A.). Each solution was degassed and thermostated by a ThermoVac accessory before the titration experiment. A constant volume of host solution in a 0.250 mL syringe was injected into the reaction cell charged with a guest molecule solution in the same aqueous solution. A control experiment was carried out in each run to determine the dilution heat by injecting an aqueous solution of the host into a pure aqueous solution containing no guest molecules. The dilution heat determined in these control experiments was subtracted from the apparent reaction heat measured in the titration experiments to give the net reaction heat. The net reaction heat in each run was analyzed by using the "Independent" model (Launch NanoAnalyze software, TA, U.S.A.) to simultaneously compute the binding stoichiometry (n), complex stability constant (K_a), standard molar reaction enthalpy ($\Delta H°$), and standard deviation from the titration curve. Generally, the first point of the titration curve was disregarded, as some liquid mixing near the tip of the injection needle is known to occur at the beginning of each ITC run. Knowledge of the complex stability constant (K_a) and molar reaction enthalpy ($\Delta H°$) enabled calculation of the standard free energy ($\Delta G°$) and entropy changes ($\Delta S°$) according to

$$\Delta G° = -RT \ln K_a = \Delta H° - T\Delta S°$$

where R is the gas constant and T is the absolute temperature. The curve fitting results for the complexation of Q[8] with different guests in aqueous solution is shown in Tables S4-S5 and Fig. S13.

Table S4. ITC profiles for the guests with Q[8] at 298.15 K

Complex	n	K_a (10^5 M^{-1})	ΔH (kJ/mol)	-TΔS (kJ/mol)
OPV^{2+}-H(1C)/Q[8]	1.028	24.670	-50.44	13.96
OPV^{2+}-Me(1C)/Q[8]	1.068	22.610	-38.38	2.11
OPV^{2+}-2Me(1C)/Q[8]	0.924	92.820	-29.83	-9.94
OPV^{2+}-H(5C)/Q[8]	0.679	11.690	-95.12	60.49
OPV^{2+}-Me(5C)/Q[8]	0.668	22.200	-88.75	52.53
OPV^{2+}-2Me(5C)/Q[8]	0.528	34.630	-69.41	32.08
OPV^{2+}-H(7C)/Q[8]	0.492	3.097	-70.92	39.59
OPV^{2+}-Me(7C)/Q[8]	0.526	1.734	-63.27	33.36
OPV^{2+}-2Me(7C) /Q[8]	0.518	1.003	-68.68	40.13

Table S5. The concentrations of guests and Q[8] host used in the ITC titrations.

	$C_{(guest)}$/mM	$C_{(Q[8])}$/mM	V/uL	Number	Interval/s
OPV^{2+}-H(1C)	1.00	0.08	10	25	250
OPV^{2+}-Me(1C)	1.20	0.08	10	25	250
OPV^{2+}-2Me(1C)	0.50	0.08	10	25	250
OPV^{2+}-H(5C)	1.00	0.09	10	25	250
OPV^{2+}-Me(5C)	1.00	0.08	10	25	250
OPV^{2+}-2Me(5C)	0.70	0.10	10	25	250
OPV^{2+}-H(7C)	0.50	0.06	10	25	250
OPV^{2+}-Me(7C)	0.60	0.08	10	25	250
OPV^{2+}-2Me(7C)	0.65	0.07	10	25	300

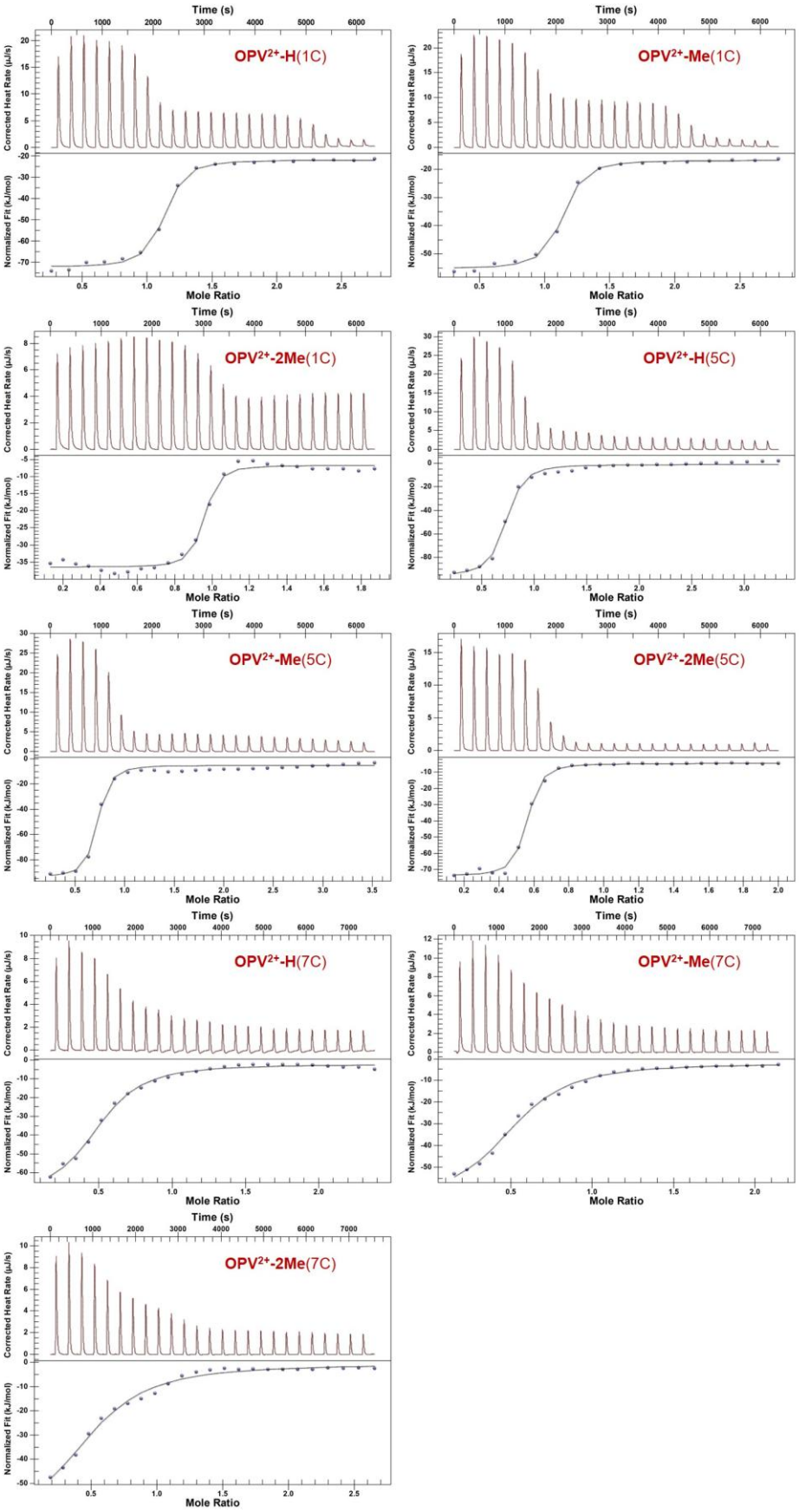

Fig. S13 ITC profiles for the guests with Q[8] at 298.15 K.

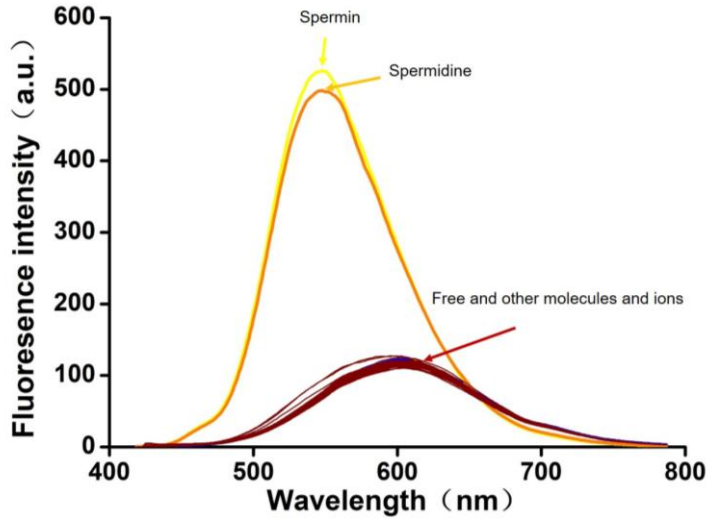

(a)

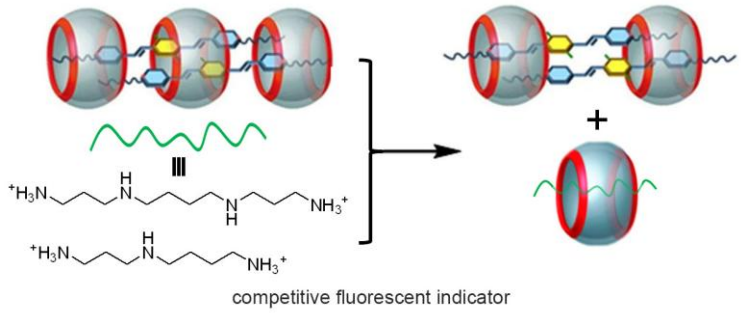

(b)

Fig. S14 (a) Fluorescence spectra of **OPV^{2+}-Me** (5C)/Q[8] (molar ration 2:3, 10.0 μM of the gust in water, pH 6.0) in the presence of various molecules (spermin, spermidine, glutathione, glutathiol, ATP, ADP, glucose, adenine, guanine, thymine, cytosine, uracil, urea, uric acid, taurine, strarch, lactic acid, glycine, L-methionine, L-Tryptophan, L-Phenylalanine, L-proline, L-Isoleucine, L-Leucine, L-Valine, L-Alanine, L-glutamine, L-asparagine, L-tyrosine, L-cysteine, L-threonine, L-serine, L-glutamic acid, L-aspartic acid, L-histidine, L-arginine and L-lysine) and ions (Li^+, Na^+, Mg^{2+}, Al^{3+}, K^+, Ca^{2+}, Cr^{3+}, Mn^{2+}, Fe^{2+}, Fe^{3+}, Co^{2+}, Ni^{2+}, Cu^{2+}, Zn^{2+}, Ag^+, Cd^{2+}, Ba^{2+}, Hg^{2+}, Pb^{2+}, F^-, Cl^-, Br^-, I^-, AcO^-, $H_2PO_4^-$, HPO_4^{2-}, PO_4^{3-}, NO_3^-, SO_4^{2-}, HSO_4^-, CO_3^{2-} and HCO_3^-) (each of 50.0 μM) in water. (b) The proposed mechanism for fluorescent recognition of spermin and spermidine.

References:

1 (a) J. Kim, I.-S. Jung, S.-Y. Kim, E. Lee, J.-K. Kang, S. Sakamoto, K. Yamaguchi and K. Kim, *J. Am. Chem. Soc.*, 2000, **122**, 540-541; (b) A. Day, A. P. Arnold, R. J. Blanch and B. Snushall, *J. Org. Chem.*, 2001, **66**, 8094-8100.

2 Y. Yang, S.Chen and X.L. Ni, *Anal. Chem*., 2015, **87**, 7461-7466.

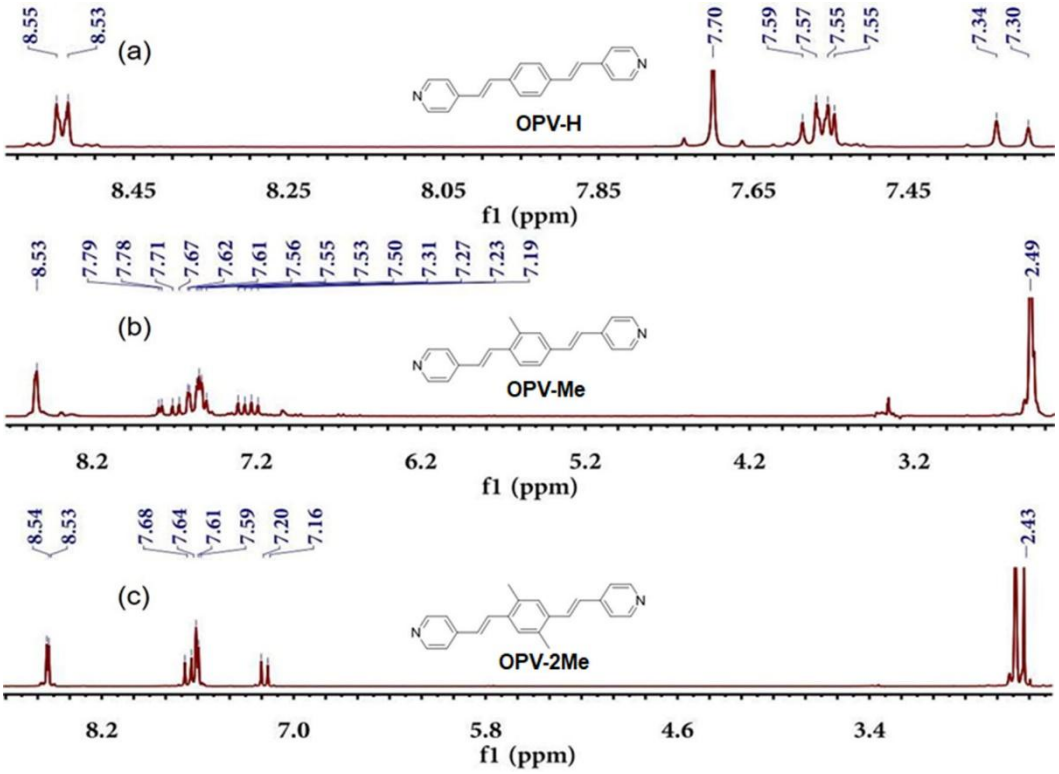

Fig. S15 ^{1}H NMR spectra (400 MHz, $DMSO_{-d6}$) of **OPV-H** (a)**, OPV-Me** (b) and **OPV-2Me** (c).

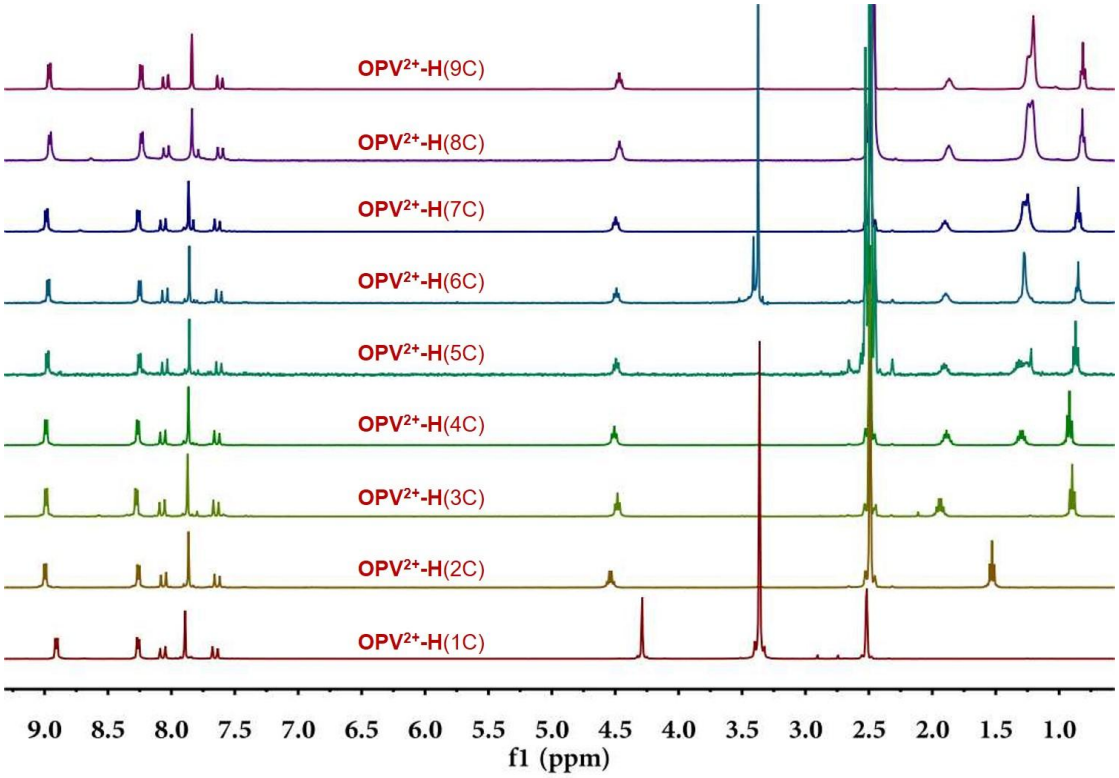

Fig. S16 ^{1}H NMR spectra (400 MHz, $DMSO_{-d6}$) of **OPV^{2+}-H** (1C-9C).

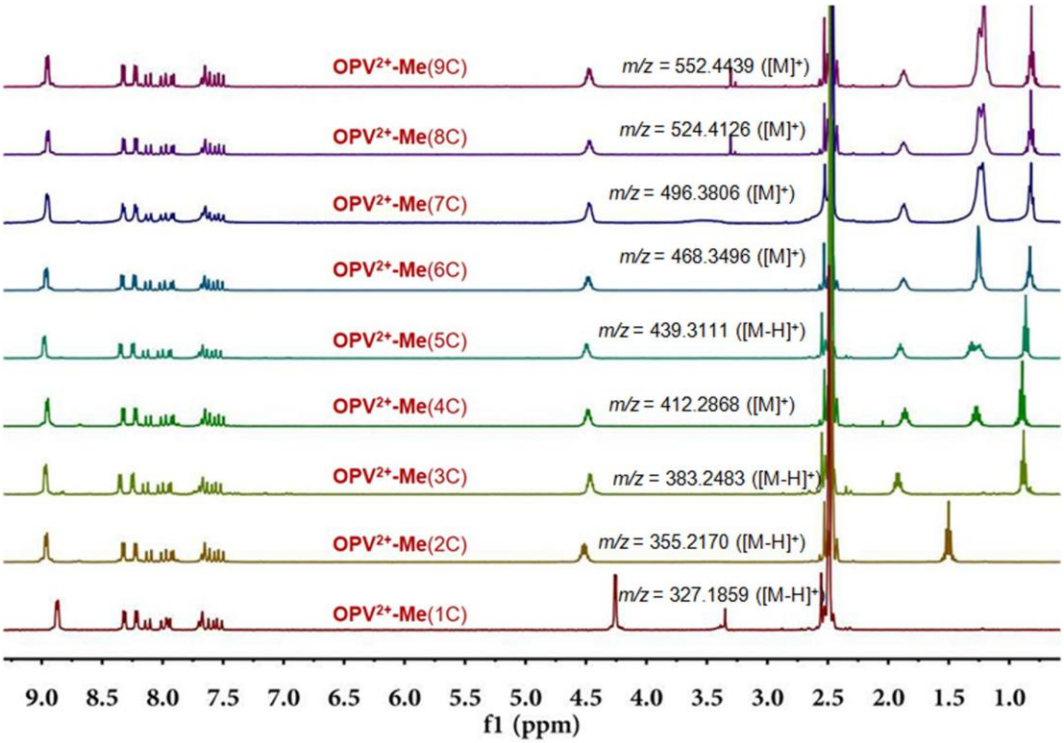

Fig. S17 ^{1}H NMR spectra (400 MHz, DMSO$_{-d6}$) and ESI-TOF MS data of **OPV^{2+}-Me** (1C-9C).

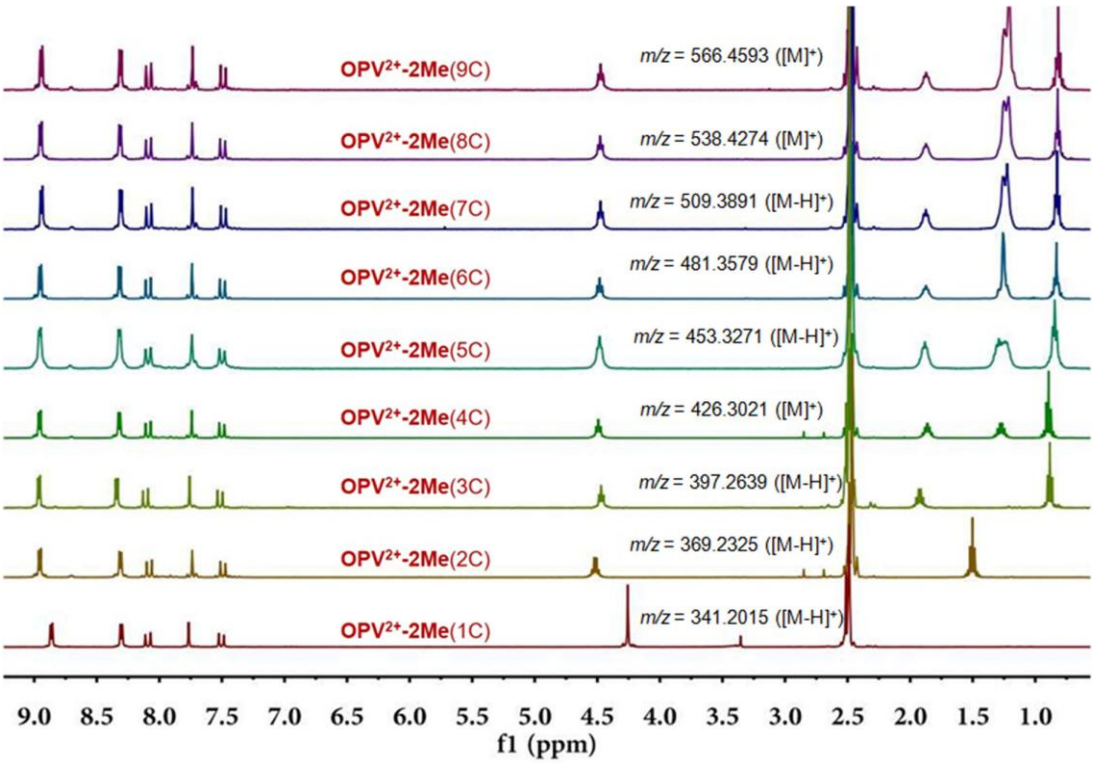

Fig. S18 ^{1}H NMR spectra (400 MHz, DMSO$_{-d6}$) and ESI-TOF MS data of **OPV^{2+}-2Me** (1C-9C).

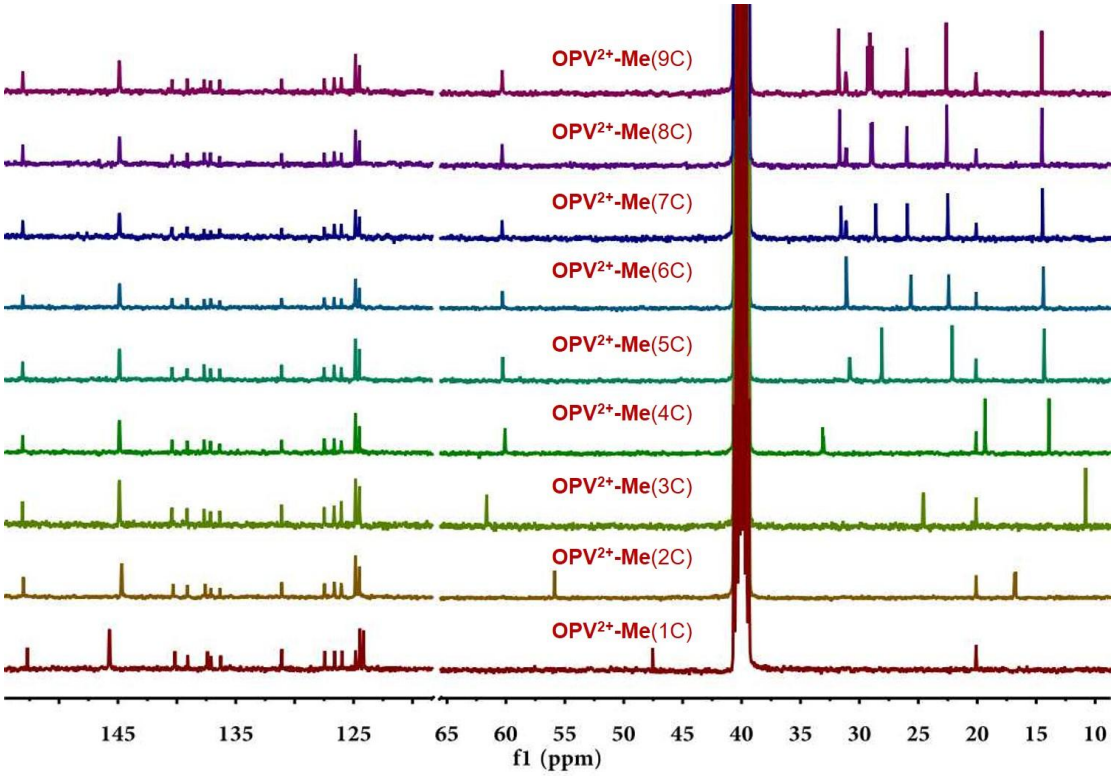

Fig.S19 ^{13}C NMR spectra (100 MHz, $DMSO_{-d6}$) of **OPV^{2+}-Me** (1C-9C)**.**

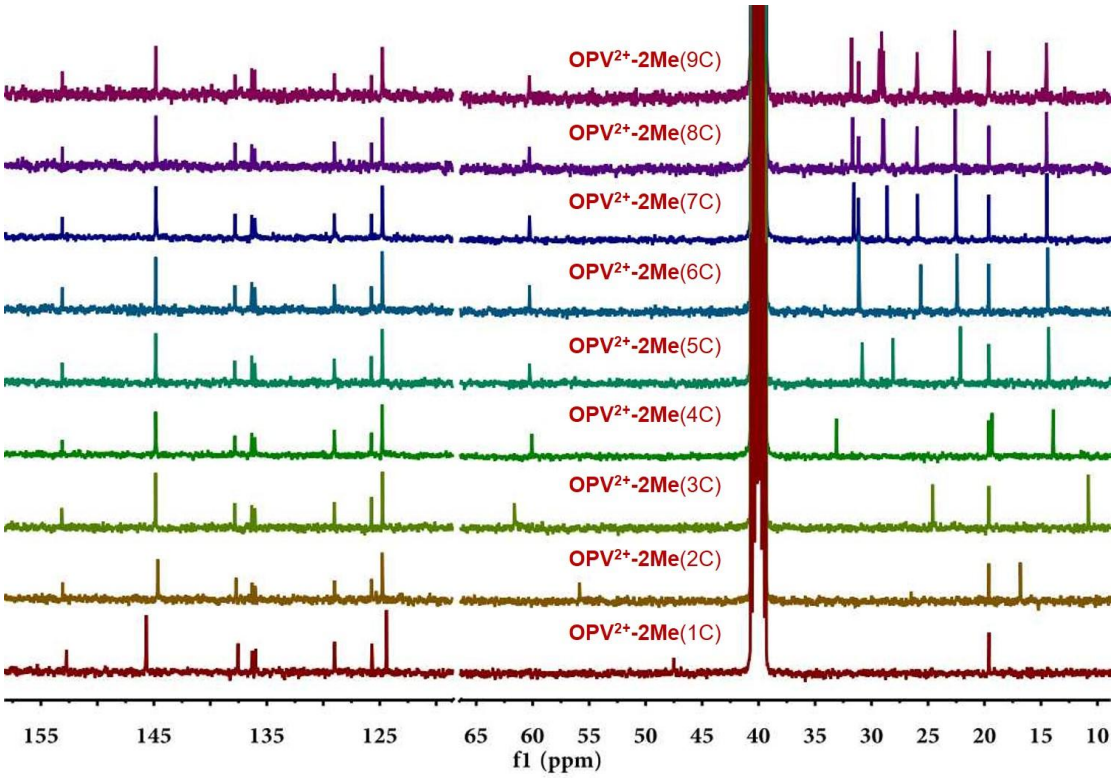

Fig.S20 ^{13}C NMR spectra (100 MHz, $DMSO_{-d6}$) of **OPV^{2+}-2Me** (1C-9C)**.**

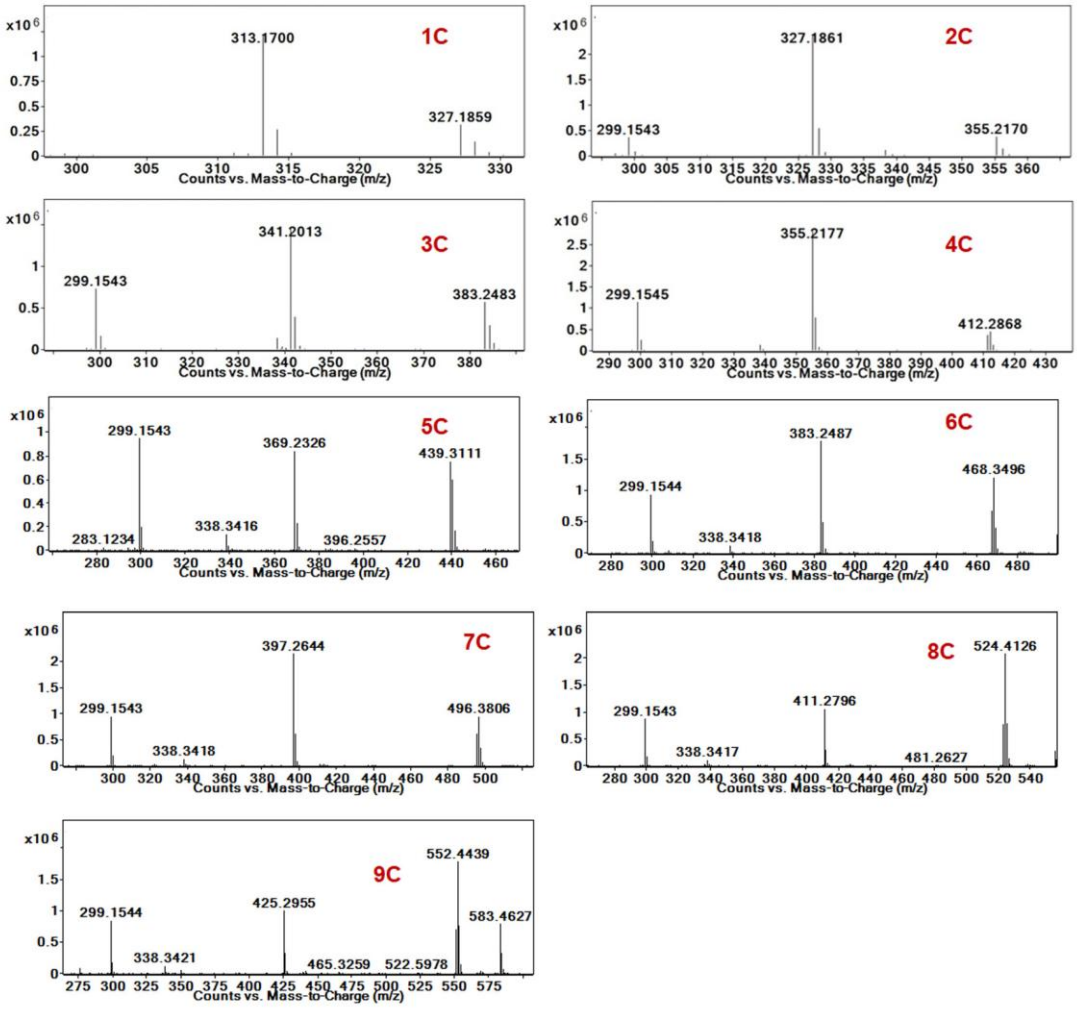

Fig.S21 ESI-TOF mass spectra of **OPV^{2+}-Me** (1C-9C) in methanol.

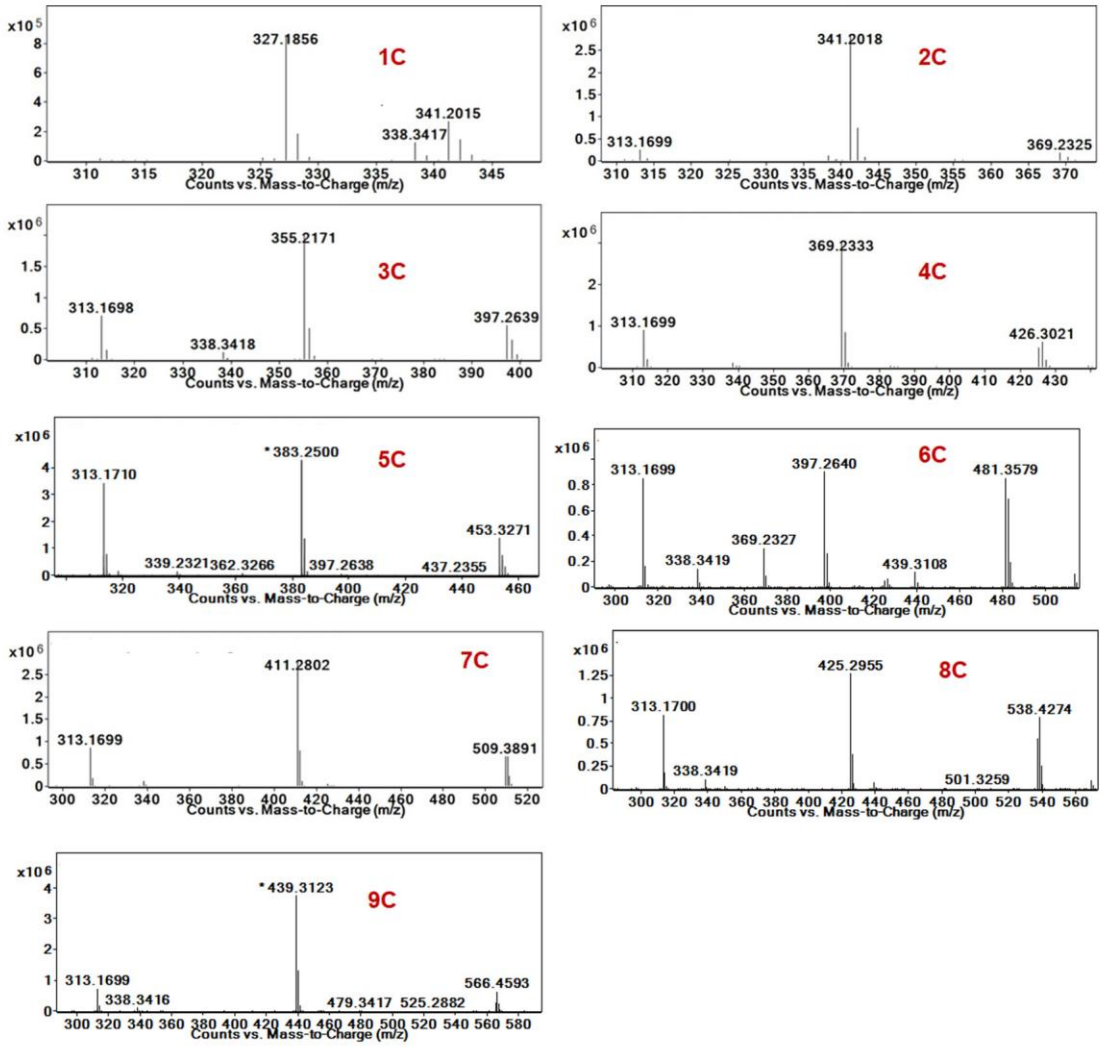

Fig.S22 ESI-TOF mass spectra of **OPV^{2+}-2Me** (1C-9C) in methanol.